



Imaging Approach to Pulmonary Infections in the Immunocompromised Patient

Shabnam Bhandari Grover^{1,2} Hemal Grover³ Neha Antil⁴ Sayantan Patra⁵ Manas Kamal Sen⁶
Deepthi Nair⁷

¹ Department of Radiology, VMMC and Safdarjung Hospital, New Delhi (Former and source of this work)

² Department of Radiology and Imaging, Sharda School of Medical Sciences and Research, Sharda University, Greater Noida, Uttar Pradesh, India (Current)

³ Department of Radiology and Imaging, Icahn School of Medicine at Mount Sinai West, New York, New York, United States

⁴ Department of Radiology and Imaging, Stanford University, California, United States

⁵ Department of Radiology and Imaging, Vardhman Mahavir Medical College and Safdarjung Hospital, New Delhi, India

⁶ Department of Pulmonary Medicine, Vardhman Mahavir Medical College and Safdarjung Hospital, New Delhi, India

⁷ Department of Microbiology, Vardhman Mahavir Medical College and Safdarjung Hospital, New Delhi, India

Address for correspondence Shabnam Bhandari Grover, MD, DNBE, MNAMS, MRCC, FICMU, FICR, E-81, Kalkaji, New Delhi 110019, India (e-mail: Shabnamgrover@yahoo.com).

Indian J Radiol Imaging 2022;32:81–112.

Abstract

Pulmonary infections are the major cause of morbidity and mortality in immunocompromised patients and almost one-third of intensive care unit patients with pulmonary infections belong to the immunocompromised category. Multiple organisms may simultaneously infect an immunocompromised patient and the overwhelming burden of mixed infections further predisposes critically ill patients to acute hypoxemic respiratory failure. Notwithstanding that lung ultrasound is coming into vogue, the primary imaging investigation is a chest radiograph, followed by thoracic CT scan. This review based on our experience at tertiary care teaching hospitals provides insights into the spectrum of imaging features of various pulmonary infections occurring in immunocompromised patients. This review is unique as, firstly, the imaging spectrum described by us is categorized on basis of the etiological infective agent, comprehensively and emphatically correlated with the clinical setting of the patient. Secondly, a characteristic imaging pattern is emphasized in the clinical setting-imaging-pattern conglomerate, to highlight the most likely diagnosis possible in such a combination. Thirdly, the simulating conditions for a relevant differential diagnosis are discussed in each section. Fourthly, not only are the specific diagnostic and tissue sampling techniques for confirmation of the suspected etiological agent described, but the recommended pharmaco-therapeutic agents are also enumerated, so as to provide a more robust insight to the radiologist. Last but not the least, we summarize and conclude with a diagnostic algorithm, derived by us from the characteristic illustrative

Keywords

- ▶ immunocompromised patient
- ▶ pulmonary infection
- ▶ CT thorax
- ▶ imaging pattern
- ▶ tissue sampling
- ▶ diagnostic algorithm

DOI <https://doi.org/10.1055/s-0042-1743418>.
ISSN 0971-3026.

© 2022. Indian Radiological Association. All rights reserved.
This is an open access article published by Thieme under the terms of the Creative Commons Attribution-NonDerivative-NonCommercial-License, permitting copying and reproduction so long as the original work is given appropriate credit. Contents may not be used for commercial purposes, or adapted, remixed, transformed or built upon. (<https://creativecommons.org/licenses/by-nc-nd/4.0/>)
Thieme Medical and Scientific Publishers Pvt. Ltd., A-12, 2nd Floor, Sector 2, Noida-201301 UP, India

cases. The proposed algorithm, illustrated as a flowchart, emphasizes a diagnostic imaging approach comprising: correlation of the imaging pattern with clinical setting and with associated abnormalities in the thorax and in other organs/systems, which is comprehensively analyzed in arriving at the most likely diagnosis. Since a rapid evaluation and emergent management of such patients is of pressing concern not only to the radiologist, but also for the general physicians, pulmonologists, critical care specialists, oncologists and transplant surgery teams, we believe our review is very informative to a wide spectrum reader audience.

Introduction

The “immune system” with innate and adaptive components is an intricate network of organs, cells, and proteins dedicated toward preventing, containing, and eradicating infective agents and cancerous mutations. Innate immunity comprises basic reflexes such as laryngeal reflex and the protective function of mucociliary clearance by intact respiratory mucosa, and neutrophils and macrophages for the entire body. The adaptive component has a humoral and cellular arm, largely controlled by lymphocytes.¹ The terminology “**immunocompromised host**” indicates a **patient** who is at an increased risk of life-threatening infections by opportunistic agents, due to either a congenital immune deficiency disease, or an acquired suppression of the immune system. **Congenital immunodeficiency diseases**, comprise a large but rare spectrum, a few examples of which are agammaglobulinemia, congenital neutropenia, Wiskott–Aldrich syndrome, and ataxia telangiectasia.^{2,3} The number of immunocompromised individuals with an **acquired suppression of the immune system** has considerably increased over the last few decades, due to human immunodeficiency virus (HIV) infection, prolific immunosuppressive therapy in patients with cancer, and in those undergoing solid organ transplants. The latter group also encompasses postsplenectomy patients, those on steroid treatment for bronchial asthma, rheumatology conditions, and collagen vascular disorders. Patients with chronic morbidity, such as diabetes mellitus, chronic alcoholism, chronic kidney disease, protein energy malnutrition and other nutritional deficiencies, obesity, and the elderly, also have an inherently low immunity.^{4–10} **The approach to immunodeficiency, therefore, requires radiologists to consider well beyond only HIV, chemotherapy, and organ transplant patients.**

A variety of usual and opportunistic infections may overwhelm an immunocompromised patient, among which the more frequent are those in the respiratory tract, skin, urinary tract, and middle ear.¹¹ The respiratory system, which is seamlessly connected to the external environment, is an easy target for opportunistic infections. The manifestation whereby an immunocompromised state is discovered is frequently in the form of **recurrent or nonresolving pneumonia**, which is also a cause of morbidity and mortality.^{4,5,12} Another aspect to be considered is that **one-third of intensive care unit (ICU) patients with pulmonary infections are immunocompromised and harbor multiple organisms**, which further predisposes them to **acute respiratory**

failure. Additionally, the incidence of **severe sepsis** characterized by systemic inflammation and acute organ dysfunction is also higher among immunocompromised patients.¹³

Although lung ultrasound as a triage technique is coming into vogue, the imaging protocol in immunocompromised patients suspected to have pulmonary infection is a chest radiograph, followed by computed tomography (CT).^{14–16} Chest radiographs provide a good screening mechanism for planning a well-tailored CT. The efficacious interpretation of the imaging studies requires an awareness of the clinical setting, duration of underlying therapy and of the associated abnormalities in other organ systems and importantly a review of the previous imaging studies. The likely organism can then be deciphered from characteristic imaging patterns.^{2,4,5,12,13,15,16} Although the final diagnosis depends on microbiological studies, imaging facilitates a fairly reliable provisional diagnosis and/or a very close differential diagnosis, for emergent initiation of therapy, which is not only lifesaving but also provides a road map for ideal sites and techniques for tissue sampling for the final diagnosis.

This review based on our experience at tertiary care teaching hospitals provides insights into the imaging spectrum of various pulmonary infections occurring in immunocompromised patients. The presented review is unique as, firstly, the imaging spectrum is categorized on basis of the etiological infective agent and emphatically correlated with the clinical setting. Secondly, a characteristic imaging pattern is emphasized in the clinical setting—imaging pattern conglomerate, to highlight the most likely diagnosis in such a combination. Thirdly, a relevant differential diagnosis is discussed in each section. Fourthly, not only are the specific diagnostic techniques for confirmation of the suspected etiological agent described, but the recommended pharmacotherapeutic agents are also enumerated, so as to provide more robust insights to the Radiologist. Last but not the least, we summarize and conclude with a diagnostic algorithm, presented as a flowchart, both from the narrative and from the typical cases illustrated.

The pathogens and immune defects: The pulmonary pathogens responsible for pneumonia in immunocompromised patients comprise of four categories and the likelihood of their occurrence varies with the type of underlying immune defect:

1. Bacterial: Nonmycobacterial and mycobacterial. The former mainly comprises *Staphylococcus aureus*, *Streptococcus pneumoniae*, *Haemophilus influenzae*, *Pseudomonas*

aeruginosa, *Klebsiella pneumoniae*, and *Escherichia coli*. The latter comprises tubercular and nontubercular mycobacteria mainly *Mycobacterium avium*–intracellulare complex or MA;

2. Fungal: *Pneumocystis jirovecii*, *Aspergillus fumigatus*, *Candida albicans*, *Cryptococcus neoformans*, mucormycosis species, *Coccidioides immitis*, and *Histoplasma capsulatum*;
3. Viruses: Cytomegalovirus (CMV), influenza, herpes simplex virus (HSV), and varicella zoster virus (VZV) and
4. Parasites: *Strongyloides stercoralis* and *Toxoplasma gondii*.

The immune defects are typically categorized as five major types, comprising of defects in phagocytosis, depressed B cell activity, depressed T cell activity, postsplenectomy immune compromise, and steroid therapy-induced immune compromise. These defects, their clinical setting and their most likely pathogens as in our experience, and that of other authors are summarized in ►Tables 1, 2, and 3.^{2,4,5,12,13,15–18}

Sampling and Laboratory Techniques for Confirmation of Etiological Agent

The ideal approach is to obtain nasal swab, sputum (expectorated or induced), blood and plasma samples, pleural fluid, and urine samples as soon as an immunocompromised patient is admitted with a suspected pulmonary infection. A dual blood culture sample from a central venous catheter along with one from a peripheral vein or from two different peripheral veins is the recommended sampling technique for immunocompromised patients. Endotracheal aspirate is obtained within 24 hours of ventilation to avoid contamination by colonizers. Fiber optic bronchoscopy and bronchoalveolar lavage (BAL) as well as transbronchial lung biopsy (TBLB) are performed to obtain lower respiratory tract samples especially in the mechanically ventilated patient and acute/chronic rejection in lung transplant recipients, suspected of having *Pneumocystis jirovecii* pneumonia (PJP). Also helpful in mediastinal lymphadenopathy is endo-bronchial ultrasound-guided transbronchial needle aspiration/biopsy (EBUS-TBNA/EBUS-TBNB). Ultrasound or CT-guided fine-needle aspiration is advised to exclude malignancy in a “non-resolving” pneumonia or to obtain samples from lung cavities suspected to harbor fungal organisms. Ultrasound guidance is preferred in lesions abutting the chest wall. **Frequent complications of all invasive procedures include hypoxemia, self-limited bleeding and pneumothorax; therefore, all invasive procedures should be performed under adequate monitoring and oxygen therapy.**^{13,17–20} Laboratory methods for the detection of pathogens isolated from respiratory samples are summarized in ►Table 4.^{21,22}

Overview: Imaging Techniques and Evaluation Protocol

Lung ultrasound, which has come into limelight since the coronavirus disease 2019 (COVID-19) pandemic, involves

screening through the intercostal spaces in 16 defined anatomical locations with a linear transducer. However, its role is limited to triage and decision making regarding the necessity of assisted ventilation in suspected COVID-19 infection.¹⁴ In all other clinical scenarios, imaging evaluation is by radiographs and CT.

Radiographic examination has a vital role to play, in the detection of a new abnormality, and for adequate follow-up. We prefer that the CT scout view also includes an overview of abdomen and pelvis, so as to quickly assess other organ systems/structures needing evaluation. A noncontrast high-resolution computed tomography (HRCT) is obtained, followed by a contrast study (in patients with normal renal parameters), which is by our protocol, extended to include the upper abdomen. On table assessment during scanning helps us to determine the necessity of extending the scans to include lower abdomen/pelvis. This is vital, as patients who are immunocompromised may have subclinical multiorgan involvement. CT pulmonary angiography (CTPA) should also be considered in patients predisposed to a complication of pulmonary gangrene, such as those with preexisting radiation pneumonitis, aspiration pneumonia, suspected fungal infections, and *Klebsiella pneumoniae*.^{23,24} Whenever a CTPA is planned, the contrast-enhanced CT is obtained as delayed phase of the study. The terminology used for description of abnormalities should be as recommended by the Fleischner Society.²⁵

The major patterns of imaging (radiographs and CT) abnormalities also broadly identify the etiological agent.

The presence of consolidation most often indicates infection with bacteria, while single or multiple nodules are usually a manifestation of septic emboli in bacterial and/or fungal infection. If a nodule is surrounded by a “ground glass halo,” then an angioinvasive fungal infection is more likely. A bronchopneumonic pattern with bronchial wall thickening, is a manifestation of certain bacteria, like *Haemophilus influenzae*. A diffuse miliary or interstitial pattern is caused either by miliary tuberculosis or by viral infections with CMV or VZV or by fungal infection with *P. jirovecii*, or *Cryptococcus*. A predominant pattern of ground-glass opacities (GGOs) is usually seen in *P. jirovecii* or in viral infections.^{2,4,5,12,13,15,16,26} It is important to bear in mind the possibility of mixed infections in immunocompromised patients, the frequently occurring examples are multi-bacterial consolidation and tuberculosis with aspergillosis coexisting in a lung cavity.

Imaging Appearances

Bacterial Pneumonia (Nonmycobacterial Organisms)

The clinical setting and presentation: All varieties of immunosuppression are risk factors for classic bacterial pneumonia, especially in patients on long-term steroid therapy and those with neutropenia or lymphopenia. The infection may be community acquired (CAP), hospital acquired (HAP), or ventilator acquired (VAP) and the symptoms comprise of acute onset cough, fever, dyspnea, and chest pain. **Staphylococcus** is a common agent; however,

Table 1 Type of immunodeficiency and most common organisms causing infection

Type of immunodeficiency	Bacteria	Fungi	Virus	Parasite
Phagocyte (first line of defense, so mucosal associated organisms usually infected) caused by steroid therapy, stem cell transplant, solid organ transplant	Usual causes of community acquired pneumonia: 1. <i>Staphylococcus aureus</i> 2. <i>Streptococcus pneumoniae</i> 3. <i>Pseudomonas aeruginosa</i> 4. <i>Klebsiella pneumoniae</i> 5. <i>Escherichia coli</i>	Usually commensals 1. <i>Aspergillus</i> 2. <i>Candida</i>	None	None
Splenectomy (nonspecific second line of defense) caused by B cell deficiency	Capsulated organisms: 1. <i>Streptococcus pneumoniae</i> 2. <i>Staphylococcus aureus</i> 3. <i>Hemophilus influenzae</i>	None	None	None
B cell defect (humoral immunity is directed against bacteria) caused by: splenectomy, hematological malignancies, myeloma	Capsulated organisms: 1. <i>Streptococcus pneumoniae</i> 2. <i>Staphylococcus aureus</i> 3. <i>Hemophilus influenzae</i> 4. <i>Pseudomonas aeruginosa</i>	None	None	None
T cell defect (granulomatous infections that is slow growing bacteria, fungi and parasites. Also Legionella, viruses as they are intracellular) caused by steroid therapy Occurs in solid organ transplant	Atypical bacteria: 1. <i>Mycobacterium tuberculosis</i> and nontubercular Mycobacteria 2. <i>Nocardia</i> 3. <i>Legionella</i>	Dimorphic fungi and yeasts 1. <i>Candida</i> 2. <i>Cryptococcus</i> 3. <i>Pneumocystis jiroveci</i> 4. Histoplasma 5. Coccidioides	Herpes group: 1. Cytomegalovirus (CMV) 2. Varicella zoster virus (VZV)	1. <i>Toxoplasma</i> 2. <i>Strongyloides stercoralis</i>
Steroid therapy: (combination of B cell and T cell immunodeficiency) and neutrophil phagocyte defect	Capsulated organisms and atypical bacteria (named above) 1. <i>Streptococcus pneumoniae</i> 2. <i>Staphylococcus aureus</i> 3. <i>Hemophilus influenzae</i> 4. <i>Mycobacteria</i> 5. <i>Nocardia</i> 6. <i>Legionella</i>	Both commensals and yeasts 1. <i>Aspergillus</i> 2. <i>Candida</i> 3. <i>Pneumocystis jiroveci</i> 4. Histoplasma 5. Coccidioides	Herpes group (same as T cell) 1. CMV 2. VZV	1. <i>Toxoplasma</i> 2. <i>Strongyloides stercoralis</i>

Note: This is based on our experience and that of the other authors.^{2,4,12}

patients with preexisting **chronic obstructive pulmonary disease (COPD), bronchiectasis, history of diabetes mellitus, smoking, and alcohol abuse are more likely to be infected with *Klebsiella*, *Pseudomonas* (the usual agent for diabetic foot), or *H. influenzae pneumonia*. Patients with HIV are also more likely to have *Streptococcus* or *H. influenzae* infection. *Mycoplasma* is a less common agent in CAP. The causative agent in VAP has been reported by Indian investigators to include *Acinetobacter baumannii* besides the above-named agents and most of these are multidrug resistant.^{2,4,12,13,15–18,27} A working knowledge of the causative agents is useful, as it helps in narrowing down the differential diagnoses.**

On radiographs and CT, most bacterial infections cause lobar consolidations, which may involve one or more segments. Involvement of multiple adjoining segments can lead to the appearance of a “**round pneumonia.**” **Staphylococcal and *Klebsiella*** infection typically cause consolidation accompanied by edema of the involved segments/lobes, resulting in **bulging of fissures.** **Staphylococcal consolidation** is usually accompanied by cavitation, bilateral pleural effu-

sions, and empyema in up to 50% patients (→**Fig. 1**). **Pneumatoceles,** with a pattern of multiple **septic emboli** and **pyopneumothorax** is another signature sign of *Staphylococcus* (→**Figs. 1** and **2**). ***Klebsiella*** infection has a tendency to occur in upper lobes and form cavities, while pleural involvement is unusual. Imaging in ***Pseudomonas* infection shows lower lobe involvement** with mixed features of multilobar consolidations, air bronchogram, and multiple areas of ground glass opacities (GGO) (→**Fig. 3**). ***H. influenzae*** infection manifests as a subsegmental or segmental consolidation with peripherally located GGOs, centrilobular nodules, and bronchial wall thickening. The consolidated segments have a tendency toward abscess formation (→**Fig. 4**). ***Mycoplasma* infection** that has a subacute onset presents with patchy nonsegmental consolidation, ground glass opacities (GGOs), bronchial wall thickening, and centrilobular nodules. Additionally, unlike *H. influenzae* infection, lymphadenopathy and pleural effusion are common.^{2,4,5,13,15,16,26,28,29}

Differential diagnosis of bacterial pneumonia: A round pneumonia may simulate a “lung mass”; however, bronchogenic carcinoma does not have an acute onset. Lobar and

Table 2 HIV-related CD-4 deficiency and type of pathogens

CD4 Count	Type of organism	Examples
>200 cells/mm ³	Community-acquired pneumonia Bacteria and some atypical bacteria	<i>Staphylococcus aureus</i> <i>Streptococcus pneumoniae</i> <i>Haemophilus influenzae</i> Primary tuberculosis <i>Legionella</i> <i>Nocardia</i>
<200 cells/mm ³	Yeasts and tuberculosis	Disseminated tuberculosis <i>Pneumocystis jirovecii</i>
<100 cells/mm ³	Atypical bacteria, commensal yeast, dimorphic fungi, viruses, parasites	NTM <i>Aspergillus</i> <i>Candida</i> Histoplasma <i>Coccidioidomycosis</i> CMV VZV Toxoplasma <i>Strongyloides</i> <i>stercoralis</i>

Abbreviations: CMV, cytomegalovirus; HIV, human immunodeficiency virus; NTM, non tubercular mycobacteria; VZV, varicella zoster virus. Note: This is based on our experience and that of the other authors.^{12,15}

segmental consolidation with edema occur in *Staphylococcus* and *Klebsiella*, but the former more often has pleural involvement. A mixed pattern of subsegmental consolidation and patchy GGOs is seen in *Pseudomonas*, *H. influenzae*, and *Mycoplasma*. *H. influenzae* and *Mycoplasma* both show interstitial opacities and bronchial wall thickening, but the differentiating feature is that the latter more often has lymphadenopathy and pleural effusion.

Laboratory confirmation of the infective agent is by examination of sputum, blood culture, and examination of BAL fluid.

Treatment: When no risk factors for drug resistance are present, ceftriaxone, doxycycline, Co-amoxiclav, macrolides, or fluoroquinolones are used as initial antimicrobial agents for a duration of 2 to 4 weeks depending on the severity.^{30,31}

Table 3 Likely pathogens in solid organ transplant

Duration posttransplant	Bacterial	Viral	Fungal
0–1 month	Gram-negative bacteria <i>Staphylococcus aureus</i> <i>Legionella</i>	HSV	<i>Candida</i>
1–6 months	<i>Nocardia</i> <i>Mycobacterium tuberculosis</i> Nontuberculous Mycobacteria	CMV RSV	<i>Aspergillus</i> <i>Pneumocystis jirovecii</i> <i>Candida</i>
3–6 months	<i>Haemophilus influenzae</i> <i>Streptococcus pneumoniae</i> <i>Mycobacterium tuberculosis</i> Nontuberculous Mycobacteria	Influenza Parainfluenza RSV	Histoplasma <i>Coccidioides</i>

Abbreviations: CMV, cytomegalovirus; HSV, herpes simplex virus; RSV, respiratory syncytial virus. Note: This is based on our experience and that of the other authors.^{12,15}

Aspiration pneumonia in immunocompromised patients as a cause of bacterial pneumonia: Patients with depressed immunity such as alcoholics and diabetic patients with cerebrovascular disease and stroke/stroke sequelae are prone to aspiration pneumonia. This is a unique entity, occurring due to accidental aspiration of gastric and oropharyngeal contents. Initially, the sterile gastric aspirate causes chemical pneumonitis that is invariably complicated by bacterial super-infection. Subsequently, rapid progression to **acute respiratory distress syndrome (ARDS)** occurs. The organisms identified in aspiration pneumonia are similar to those for community acquired pneumonia—*Pseudomonas*, *Klebsiella*, *E. coli*, and *Staphylococcus*. If there are multiple lung segments involved/extensive air-space disease, then the **likelihood of multiple organisms, drug resistance, ARDS, necrotizing pneumonia, and lung gangrene increases.**^{32–34}

Radiographs and CT show **consolidation usually in bilateral lower lobes** (gravity-dependent lung segments), if the patient aspirates in an upright posture (→Fig. 5). However, **alcoholics** are more likely to aspirate in a prone posture and are therefore more likely to have right **upper lobe involvement**. Urgent recognition by radiologists is imperative, so that emergent aggressive lifesaving therapy with antibiotics and assisted ventilation may be instituted.^{32,33}

Laboratory confirmation of the infective agent is by a protocol similar to that for CAP. **Empirical treatment** with antimicrobial is dependent on the site of acquiring aspiration pneumonia community/hospital and risk factors for infection with multidrug resistant organisms. For community-acquired infection, ampicillin-sulbactam, carbapenem, or quinolone may be appropriate. Where anaerobic infection is suspected (lung abscess, necrotizing pneumonia, periodontal disease), clindamycin is used.^{17,18,33}

Necrotizing Pneumonia: A Dreaded Complication of Bacterial Pneumonia

While any bacterial pneumonia may progress to a rare and potentially fatal complication of necrosis and gangrene, a greater likelihood is present in patients with coexisting sepsis, and in those with extensive and multilobar airspace opacities.³⁴ The CT signs of necrotizing pneumonia are

Table 4 Diagnostic tests for specific pathogens

Pathogen	Microbiology diagnosis
Pyogenic bacteria (<i>Staphylococcus</i> , <i>Streptococcus</i> , EGNB)	<ol style="list-style-type: none"> 1. Direct demonstration on Gram stain 2. Culture in dedicated solid media, like blood agar (for gram-positive bacteria) and MacConkey agar (gram-negative bacteria) 3. Phenotyping and antimicrobial susceptibility using automated techniques (API or VITEK) or biochemical analysis
<i>Mycobacterium tuberculosis</i> complex and NTM	<ol style="list-style-type: none"> 1. Direct demonstration on acid fast staining 2. Automated culture methods—MGIT or BacT/ ALERT 3D 3. Phenotypic methods (MPT 64 antigen assay) 4. Line probe assay 5. Rapid detection using cartridge-based nucleic acid amplification technique (CBNAAT) or TrueNat 6. Liquid culture and sensitivity for advanced susceptibility testing
Fungal agents	<ol style="list-style-type: none"> 1. Direct examination by staining with Giemsa, India ink or Gram stain 2. Culture on Sabouraud's dextrose agar (SDA) or blood agar
Aspergillus	Rapid antigen detection using Galactomannan assay and panfungal reverse transcription polymerase chain reaction (RT-PCR)
Histoplasma and <i>Coccidioides</i>	<ol style="list-style-type: none"> 1. Direct smear 2. RT-PCR
Viruses	<ol style="list-style-type: none"> 1. RT-PCR 2. Immunofluorescence
Parasites	Direct staining of biopsy or aspirates using Giemsa or Wright stain

Abbreviations: EGNB, enteric gram negative bacteria; NTM, non tubercular mycobacteria.

multiple small abscesses with nonenhancing foci in consolidated lung. In case the nonenhancing areas exceed 50% of the involved lobe, along with obliteration/thrombosis of the regional pulmonary vascularity, pulmonary gangrene is most likely present (► Fig. 6). As both necrotizing pneumonia and gangrene have significant high mortality, the radiologist's acumen becomes a critical link. **Diligent evaluation of the pulmonary vasculature and excluding hypo/nonenhancement of consolidated lung** is necessary to exclude pulmonary gangrene (► Fig. 6). **Aggressive medical treatment** is often necessarily supplemented by debridement, wedge resection, and/or lobectomy.³⁴

Mycobacterial Infection in HIV and Other Immunocompromised Patients

The clinical setting and presentation: In high endemicity countries, tuberculosis occurs frequently in all groups of immunocompromised patients: those **with mild immunosuppression such as diabetes and alcoholism** as well as in those with moderate suppression as in **prolonged steroid therapy**, and severe suppression such as **cancer, solid organ transplant, tumor necrosis factor- α antagonist therapy, and HIV infection**. It is known that, with highly active antiretroviral therapy (HAART), longevity of HIV-afflicted patients has considerably improved; however, they are at a 50- to 200-fold greater risk compared with the general population to **develop tuberculosis at any stage**.⁴ Symptomatology ranges from low- to high-grade fever, cough, night sweats, weight loss, dull chest pain, and pleuritic pain.¹³

Imaging appearance: The radiological pattern of involvement differs significantly in immunocompromised

patients with tuberculosis, compared to their immunocompetent counterparts. In immunocompromised patients, lower lobe involvement is commoner than upper lobe. In HIV patients, as long as CD-4+ counts are above 350 cells/ μ L, the CT pattern is of postprimary/reactivated tuberculosis, similar to non-HIV patients. Appearances are of nonlocalized, cavitating consolidation of **lower lobes**, often surrounded by **centri-lobular "tree-in-bud" nodules**. Mediastinal lymphadenopathy is often associated with faint peripheral or rim enhancement and central nonenhancing necrotic areas (► Figs. 7, 8, and 9). Pleural effusion is common. **Severely immunocompromised patients with CD4+ counts below 200 cells/ μ L are more frequently known to present like a primary tuberculosis with miliary and disseminated pattern of disease and a fulminant course (► Fig. 10).**^{15,35} Miliary tuberculosis manifests on CT as multiple <5 mm random nodules (► Fig. 10). A few of these nodules may have sharp and others may have unsharp margins. The interlobular septa are thickened and few areas of GGO may also be present. Pleural effusion may accompany miliary tuberculosis as well.^{15,35} **In both manifestations of tuberculosis, abdominal organs should also be surveyed.**

In postprimary type of lung involvement, lesions in liver, spleen, and adrenal are macronodular, whereas in the primary type of manifestation with miliary tuberculosis in lungs, the liver, spleen, and adrenal gland also show miliary lesions. Ascites and abdominal lymphadenopathy are likely in both forms of the disease.^{36,37}

The differential diagnoses for postprimary tuberculosis includes fungal infection (invasive aspergillosis and/or

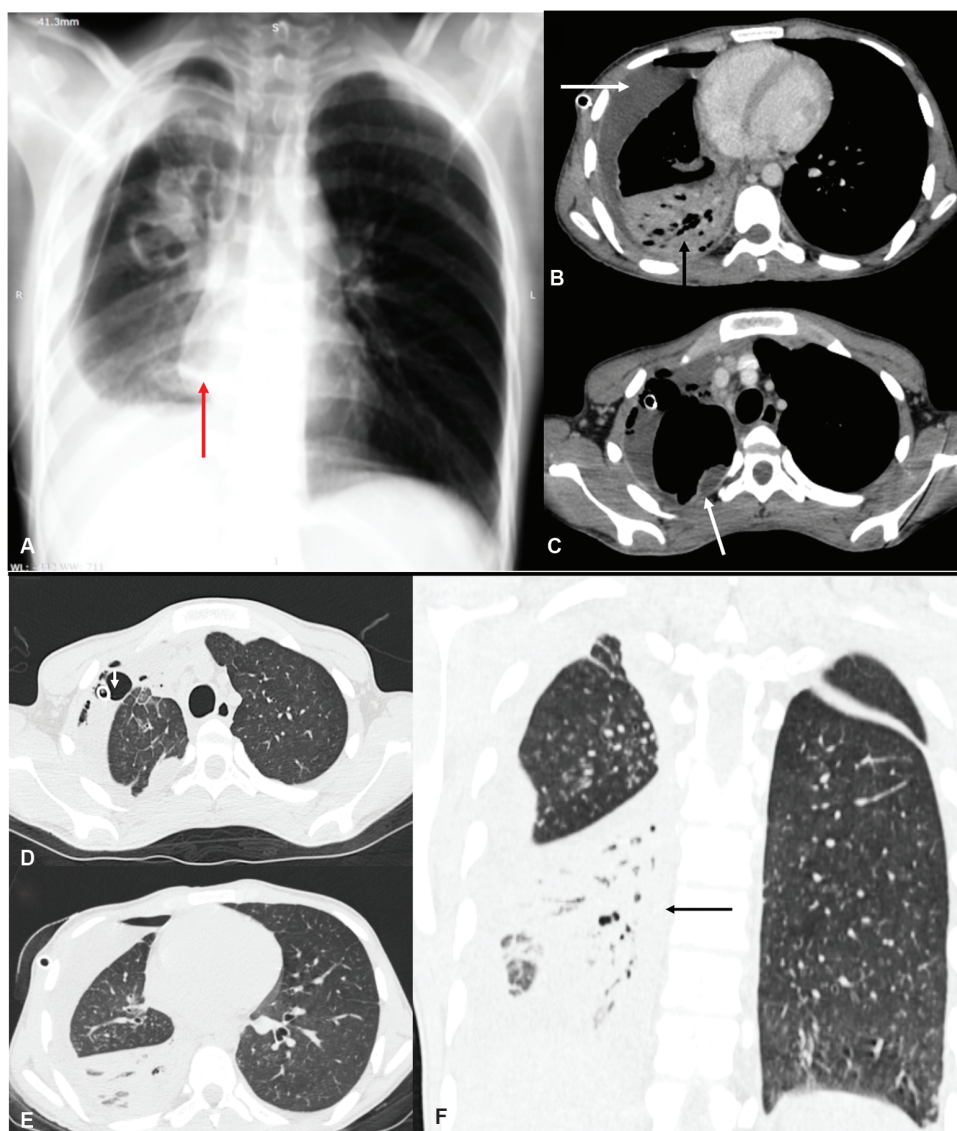


Fig. 1 Imaging studies of thorax in a diabetic male aged 18 years, with fever, cough, and chest pain for a week. Chest radiograph (A) shows right retrocardiac density (red arrow) and right hydropneumothorax with drainage tube. Contrast-enhanced computed tomography (B–F) shows right pyopneumothorax (white arrow) (B), with right lower lobe consolidation with air bronchogram (black arrow) (B), with early involvement of left posterior basal segment (black arrow) (F). Lobar consolidation with pyopneumothorax is characteristic for staphylococcal pneumonia. *Staphylococcus* was grown in blood culture.

candidiasis) and *Mycoplasma pneumoniae*. The clinical setting is of chronic symptoms and diabetes, HIV or steroid therapy for tuberculosis, acute onset and hematological malignancies for angioinvasive *Aspergillosis/Candidiasis* and of subacute onset and chronic alcoholism and/or diabetes for semi-invasive aspergillosis, histoplasmosis, and mucormycosis. **In our experience, presence of lymphadenopathy and pleural effusion often points toward tuberculosis.** Although the liver and spleen are involved not only in tuberculosis but also in aspergillosis and candidiasis, associated involvement of the **adrenal gland** with abdominal lymphadenopathy and ascites favors tuberculosis.³⁷ **Occasionally, adrenal gland involvement also occurs in disseminated histoplasmosis,** but pleural effusion and ascites are relatively less common in histoplasmosis.^{38,39} A miliary

pattern of nodules may also be seen in viral infections, but in viral etiology, usually a halo is present around nodules, along with GGO and an interstitial pattern.¹⁵

Diagnosis is confirmed by sputum smear and culture or by documenting acid fast bacilli in aspirated pleural fluid or from the fluid obtained by BAL. The **recommended treatment** is as per World Health Organization and Revised National Tuberculosis guidelines as per the NTEP (National Tuberculosis, Elimination Program), India. For a freshly diagnosed case, four drugs in the initial 2 months phase include rifampin, isoniazid (INH), ethambutol, and pyrazinamide. After 2 months, pyrazinamide is withdrawn and the rest are continued for a further period of 4 months.^{40,41} The necessity for further treatment is decided on an individual case need basis.

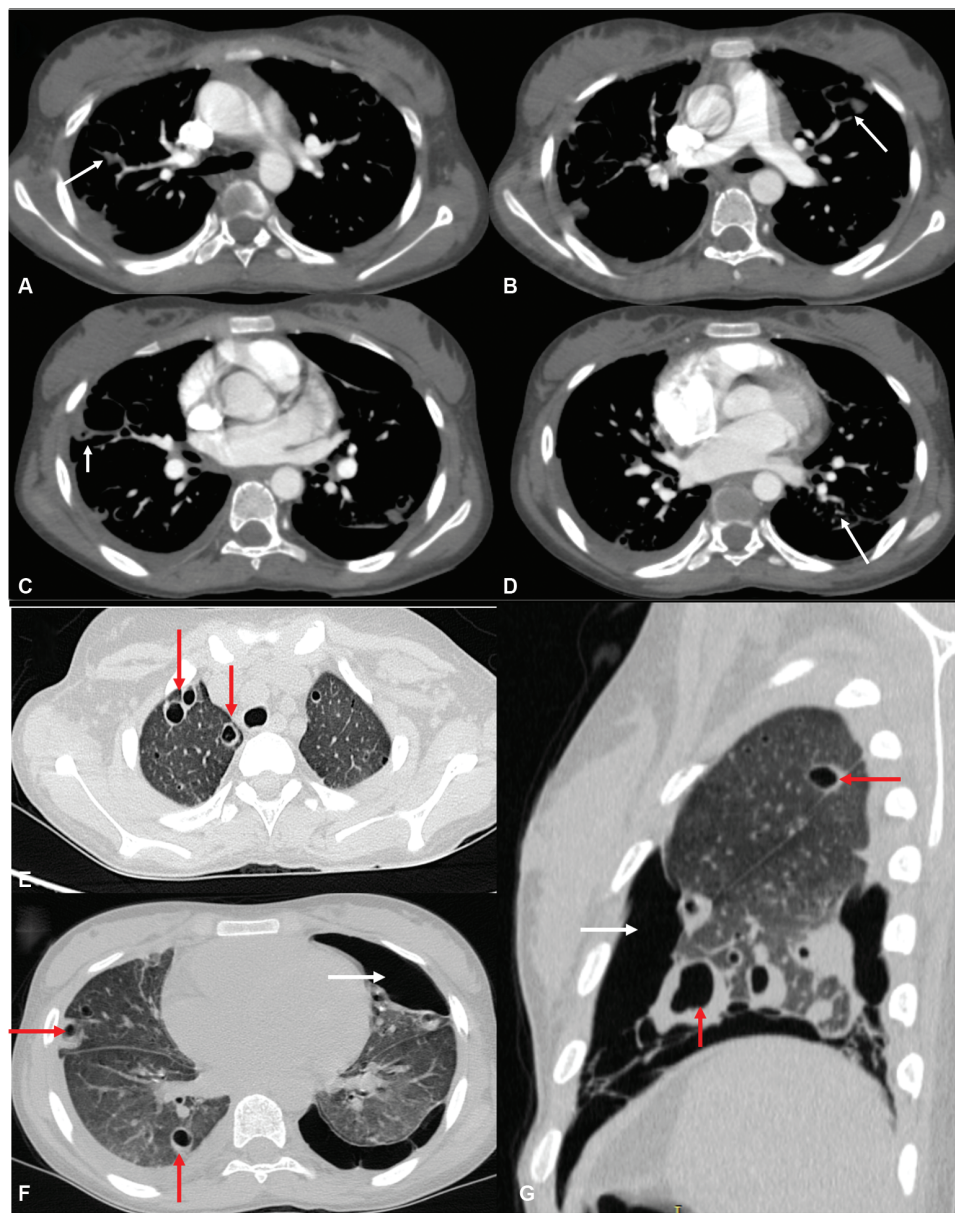


Fig. 2 Computed tomography (CT) of a 15-year-old girl who was on immunosuppressive therapy for aplastic anemia, with a history of cough, fever, tachypnea, and chest pain for a week. Scout view had shown multiple nodular lesions; therefore, CT pulmonary angiography (CTPA) was performed to rule out septic emboli in the pulmonary circulation. CTPA (A–D) shows normal pulmonary vasculature, but multiple lung nodules with feeding vessels (white arrows). Lung windows (E–G) show multiple pneumatoceles (red arrow) and left-sided pneumothorax (white arrow), characteristic of *Staphylococcus* infection. The suspected organism was grown in sputum culture.

Fungal Infections

Overview of Various Invasive Infections and Their Typical Clinical Associations

The type of fungal infection that develops in an immunocompromised patient depends on the type of immunosuppression. **Angioinvasive fungal infection** is more likely in patients **on prolonged high-dose steroids, patients of solid organ or bone marrow transplant, those with hematological malignancies, those on immunosuppressive chemotherapy, and in patients at the end stage of HIV/AIDS.** *Aspergillus* and *Candida* are the most frequent pathogens in angioinvasive disease. **The symptoms include fever, cough, and dyspnea, but there is characteristically a lack of**

response to an adequate dose and duration of broad-spectrum antibiotics. Febrile neutropenia, occasionally with hemoptysis, is a typical setting for angioinvasive fungal infection in immunocompromised patients.⁴²

Semi-invasive or chronic necrotizing aspergillosis is clinically associated with diabetes, alcoholism, malnutrition, advanced age, prolonged steroid therapy, and COPD. Infection by **mucormycetes** (mucormycosis, previously called zygomycosis) is next in frequency and is the pathogen in patients with **uncontrolled diabetes and prolonged steroid therapy.** These patients usually have associated rhinocerebral lesions. **Histoplasmosis** is another likely agent in patients with **diabetes and HIV.** Histoplasmosis usually occurs along the Gangetic plains of India, which are infested

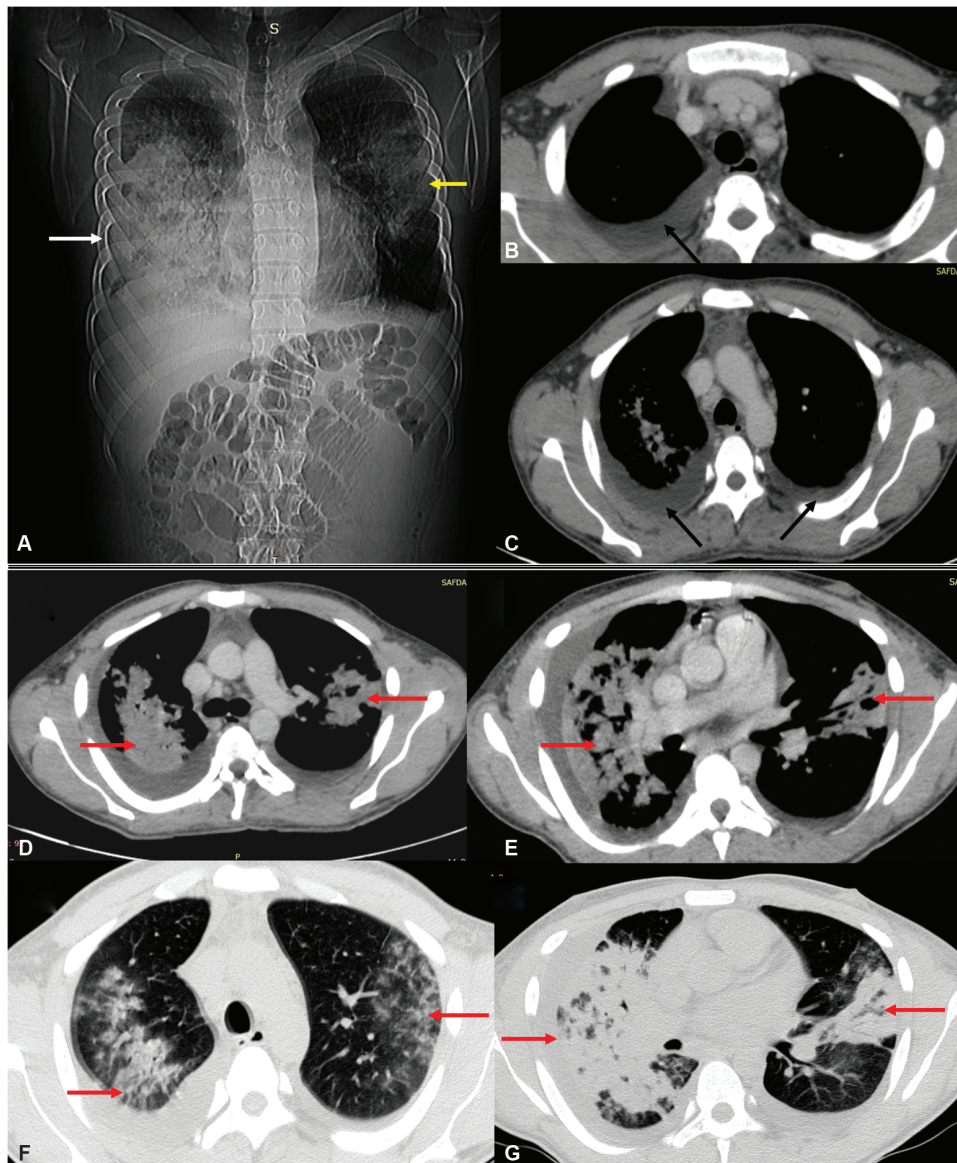


Fig. 3 Computed tomography of a 22-year-old male, chronic alcoholic, with recent high-grade fever, cough, and respiratory rales. Scout view (A) shows right lower lobe consolidation (white arrows) with bulging horizontal fissure and infiltrates in left lung (yellow arrow). The contrast-enhanced computed tomography study shows bilateral pleural effusion (black arrows), paratracheal lymphadenopathy (B, C). Lung windows (D–G) show extensive, bilateral patchy consolidation, with air bronchogram (red arrows). Imaging features suggest mixed bacterial infection. *Pseudomonas* and *Staphylococcus* were both grown in blood culture.

with bird and bat droppings. Patients usually present with mucocutaneous lesions and chronic lung disease. **Cryptococcosis also occurs in HIV patients, hematological malignancies, and solid organ transplant patients.**^{38,42–44}

PJP is a fungal pulmonary infection that occurs in severely immunocompromised patients, such as HIV with low CD-4 counts <100 cells/mm³, organ transplant recipients, and those with hematopoietic stem cell transplant. *P. jirovecii* in immunocompromised patients has a predilection to infect the lung due its ability to attach with type 1 alveolar epithelium. This characteristic allows it to transition from a small trophic form to a large cystic form and further to disseminated disease. A unique feature about PJP is that the disease is more fulminant in non-HIV immunosuppressed patients than in HIV patients.^{42,45,46}

Blastomycosis is endemic in the geographic locations adjoining the south, central, and mid-west river regions of America; these regions are rich with deadwood and moist soil. This disease, therefore, more often **affects immunocompetent men** who are involved in forest activities. However, when it occurs **in immunocompromised, the manifestations are severe.** The disease has been reported sporadically from India as well.^{47,48}

Radiological and Imaging Features of Aspergillus and Candida

Four distinct manifestations (types 1, 2, 3, and 4) are known for *Aspergillus*-associated pulmonary disease. Type 1 and 3 occur in immunocompetent patients. Type 1 is a simple *Aspergilloma* occurring as saprophytic superinfection in a

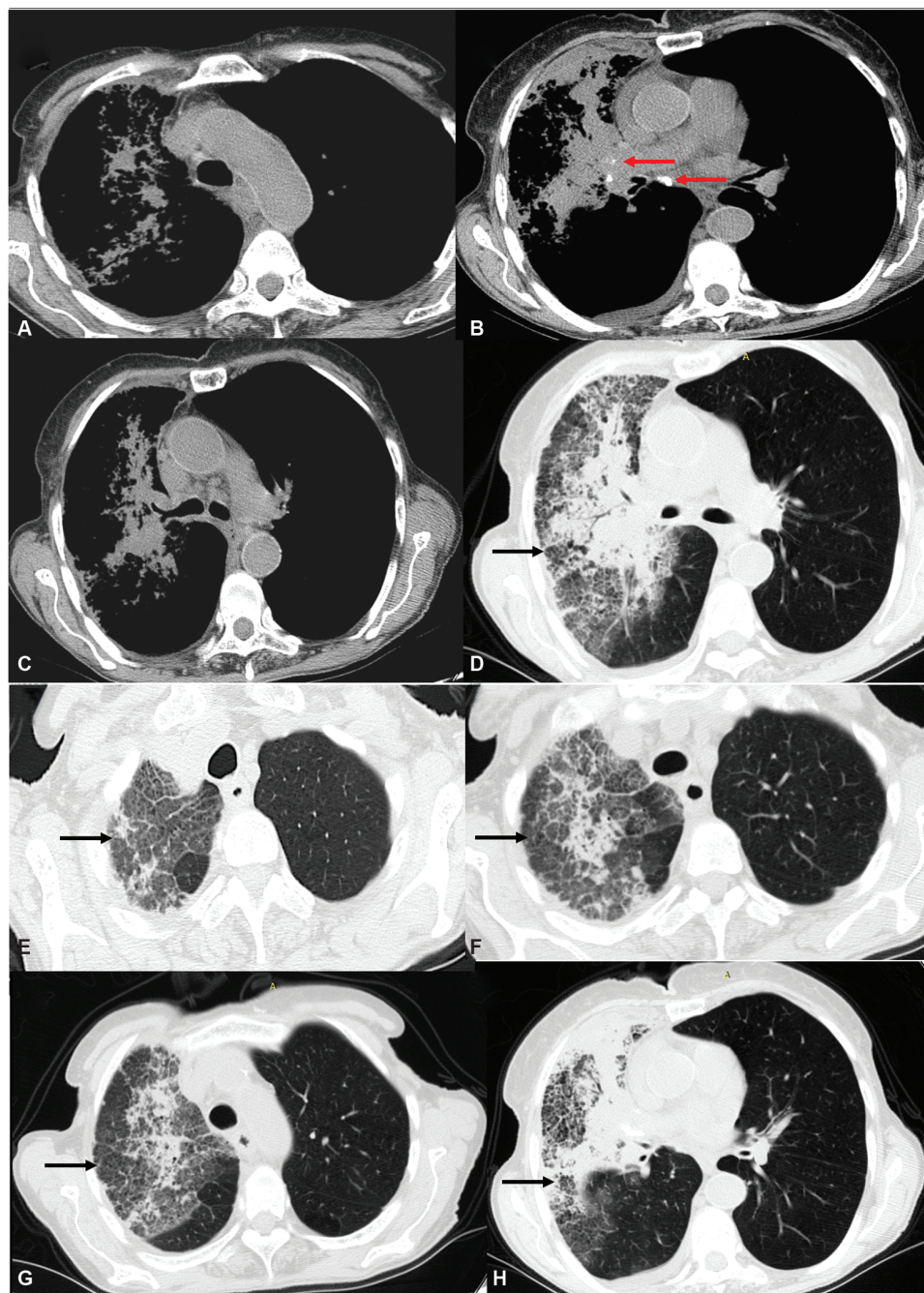


Fig. 4 Computed tomography (CT) study in a 75-year-old diabetic male, smoker with fever, cough, breathlessness, not responding to broad-spectrum antibiotics. CT shows old volume loss in right lung with calcified nodes (red arrow) (A–C). Lung windows (D–H) show a mixed pattern of disease, with patchy segmental consolidation and ground glass opacification in right lung. There is evidence of bronchial wall thickening in the form of reticular shadows. The entire imaging spectrum is characteristic for *Hemophilus influenzae*. The suspected organism was grown in blood culture.

preexisting cavity or bronchiectasis (►Fig. 11). Type 3 is an allergic noninvasive aspergillosis. **Type 2 and 4 both occur in immunocompromised patients. Type 2, which is chronic pulmonary aspergillosis,** occurs in mildly immunocompromised patients, such as those with diabetes, alcoholism, and steroid intake. A distinct variety of chronic pulmonary aspergillosis known as **chronic necrotizing aspergillosis exhibits local invasion** into adjoining pleura and chest wall and has been very aptly described by Greene as “a regionally destructive lung process” (►Fig. 12). **Type 4, the invasive**

form, (►Figs. 13, 14, and 15) **comprising both angioinvasive and airway-invasive varieties, occurs in moderate to severely immunocompromised patients especially those with hematological malignancies.**^{49,50}

The imaging features of subacute or chronic infection with aspergillosis (the type 2 form) and *Candida* are almost similar, resemble tuberculosis, and comprise a mixed pattern of nodular opacities and patchy consolidation on radiographs and/or CT (►Fig. 12). Cavitation is sometimes observed. HRCT may show “tree-in-bud” centrilobular nodules

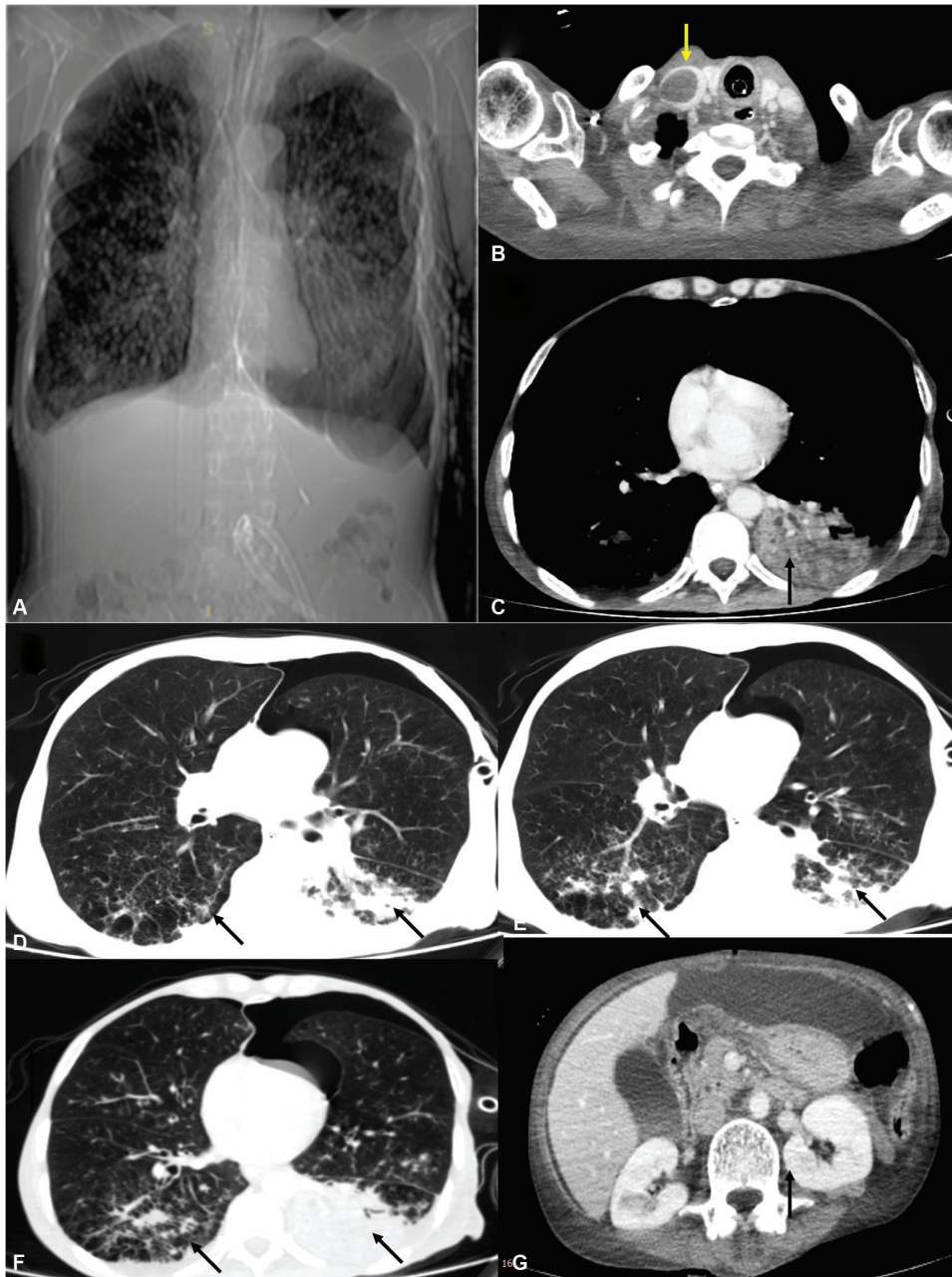


Fig. 5 (A–G) Computed tomography (CT) of a 60-year-old male on prolonged steroid therapy for asthma. Recent surgery for duodenal perforation, followed by respiratory distress. Scout view shows chronic obstructive pulmonary disease, with bilateral lower lobe infiltrates. Contrast-enhanced computed tomography (B) shows thrombus in right internal jugular vein (yellow arrow), left lower lobe consolidation (black arrow) (C). Lung windows (D–F) show bilateral lower lobe opacities (black arrows), confirming aspiration. Upper abdomen reveals coexisting pyoperitoneum (G), all findings of multifocal infection and septicemia. The blood culture grew mixture of *Staphylococcus*, *Streptococcus*, and *Klebsiella* organisms.

and nonsegmental consolidation with ill-defined margins that may have air bronchograms. Lymphadenopathy and pleural effusion may accompany the parenchymal abnormalities. **A clue to the likelihood of a fungal infection is the propensity for local invasion into the chest wall. Associated paranasal sinus involvement is another characteristic feature of *Aspergillus* infection, especially in patients with febrile neutropenia.**^{49–56}

Angioinvasive disease (type 4) may occur with both aspergillosis and candidiasis, and the early HRCT sign is the presence of a single or multiple macronodules (>1 cm), surrounded by GGO,

popularly christened the “CT halo sign.” A “reverse halo sign” is also an indicator of invasive fungal infections and comprises an area of GGO, surrounded by consolidation. The **macronodule** is believed to be the central infective nidus and the GGO is due to thrombosis and hemorrhage in the surrounding alveoli. **Multiple macronodules without halo** are also indicative of angioinvasive aspergillosis (–Figs. 13 and 14). Patchy wedge-shaped subpleural consolidation later develops (which indicates infarction), appears as a “hypo-enhancing” area and subsequently undergoes necrosis and cavitation (–Fig. 16). The **recovery phase** is marked by retraction of the infarcted tissue from its wall, forming

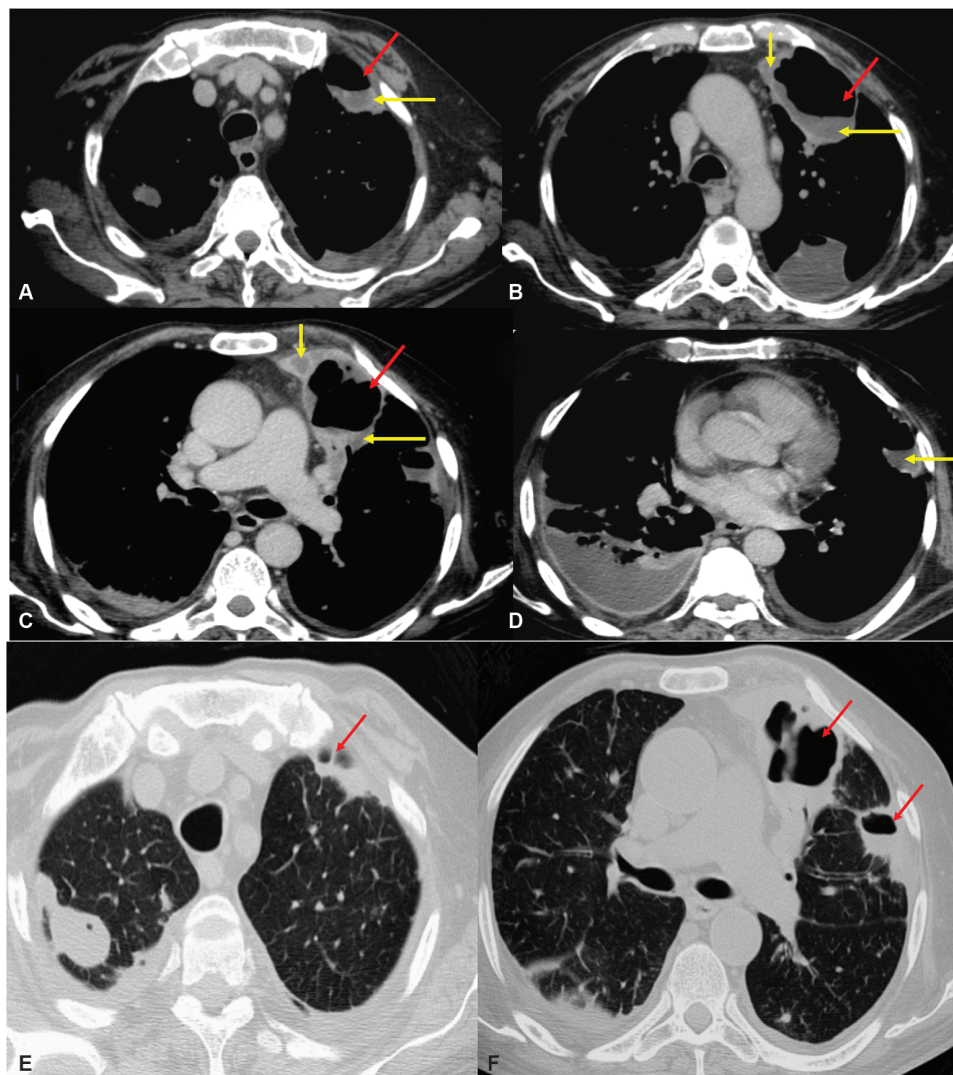


Fig. 6 (A–F) Computed tomography of a 57-year-old male, with uncontrolled diabetes, cough, fever, and respiratory distress for the last 2 weeks. Contrast-enhanced computed tomography mediastinal window (A–D) shows multiple segments of necrotizing consolidations (red arrows), seen as hypoenhancing lung parenchyma (yellow arrows), although pulmonary vasculature does not show any cut off. Bilateral empyema is present. Lung windows (E, F) show cavitating consolidation (red arrows), but hypoenhancement of consolidated lung is seen only on mediastinal windows. Blood culture grew *Streptococci* and *Staphylococci*, both known to cause necrotizing pneumonia.

a cavity and giving rise to the “air crescent sign” or “Monod sign” (► Fig. 15). Other patterns of manifestation are, a mixed pattern with macronodules and a halo sign, miliary nodules, centrilobular tree in bud nodules and wedge shaped pleural based consolidations.^{49–56} Although pleural effusion is less frequently reported, we have observed it in a few patients (► Figs. 13 and 14).

Differential diagnosis of the lung lesions: A mixture of nodular opacities and patchy consolidation seen in the subacute or chronic form of disease resembles reactivated tuberculosis. The “halo sign” and “reverse halo sign” seen in angioinvasive disease can be seen in other fungal infections, and much less frequently in tuberculosis, parasitic infestations, hemorrhagic metastases, Kaposi’s sarcoma, and polyangiitis causing entities and cryptogenic organizing pneumonia.^{42,51–56} **Therefore, correlation with the clinical setting and the immune status of the patient is necessary to arrive at an accurate diagnosis.**

Most fungal infections including aspergillosis may very often be a clinically silent disseminated disease, unraveled only on imaging. Therefore, in all patients suspected to have aspergillosis or candidiasis, CT is extended to include the abdomen. Both these organisms, more frequently, *Candida*, invade the hepatobiliary and gastrointestinal system and the peritoneum by hematogenous dissemination. *Candida* and aspergillosis lesions in the liver have myriad presentations ranging from microabscesses/miliary foci <5 mm to nodules and large granulomas with peripheral rim enhancement. Hepatic candidiasis lesions are typically described on ultrasound as “bull’s eye” or “spoke wheel” and are seen to have a hyperattenuating center on noncontrast CT, due to fungal hyphae. We have seen microabscesses in the liver, both with disseminated aspergillosis and disseminated candidiasis (► Figs. 15 and 16). The bowel wall may show concentric wall thickening, with nodular infiltration of peritoneum and retroperitoneum.⁵⁷ Associated abdominal invasion should

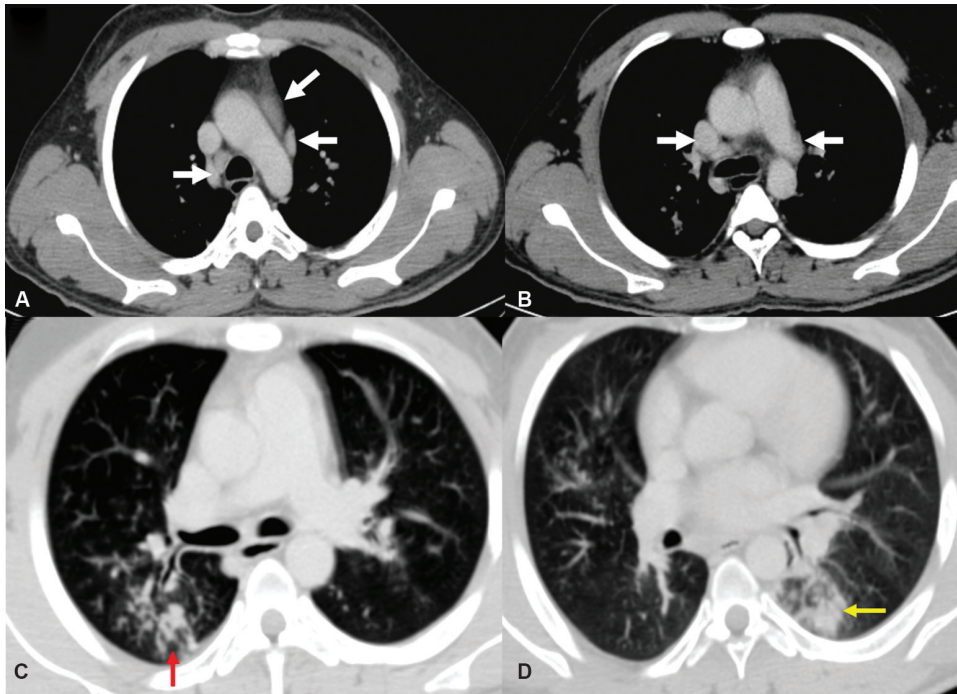


Fig. 7 (A–D) Contrast-enhanced computed tomography in a 25-year-old male on immunosuppressive treatment for aplastic anemia, who developed acute onset high-grade fever and respiratory distress. Mediastinal windows (A, B) show faint but homogeneously enhancing pretracheal lymph nodes (white arrows). Lung windows (C, D) show “tree in bud” opacities in right lung (red arrow) and patchy consolidation in left lung (yellow arrow). These variegated imaging appearances are characteristic for tuberculosis. The sputum smear examination confirmed tuberculosis.

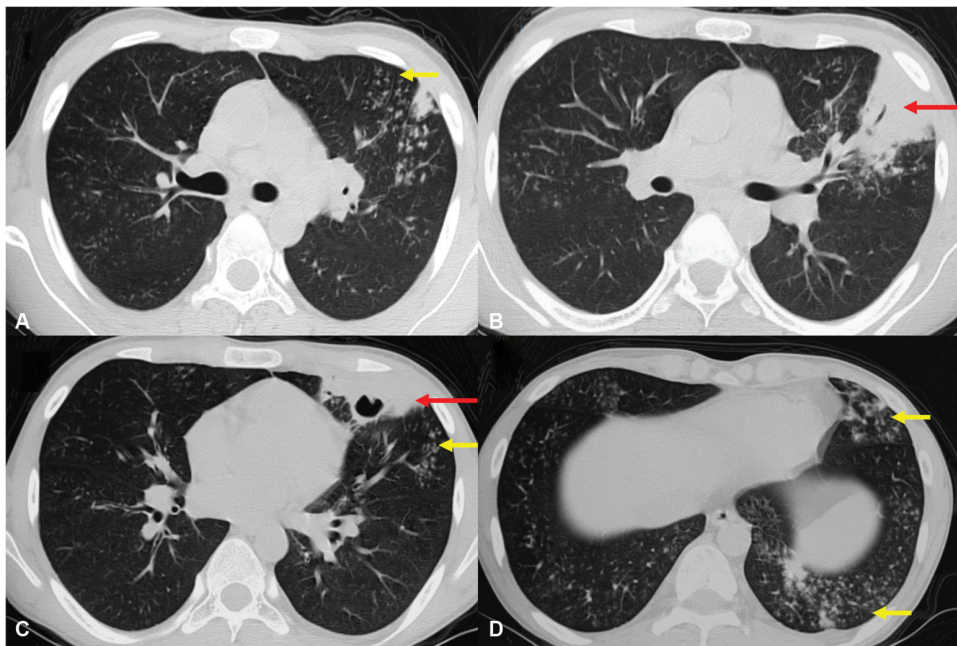


Fig. 8 (A–D) Noncontrast computed tomography in a 18-year-old male, a known case of systemic lupus erythematosus, on prolonged steroid therapy, with complaints of fever, cough, chest pain and his renal functions were deranged. Lung windows show “tree in bud opacities” (yellow arrows) along with segmental consolidation in left lingular lobe (red arrows). The imaging appearances are characteristic for tuberculosis. Sputum smear confirmed tuberculosis.

be excluded as disseminated disease worsens the prognosis..

The diagnosis is confirmed by a combination of sputum analysis, enzyme-linked immunosorbent assay of blood samples, and BAL aspirate cytology, whereas histopathology

of lung tissue is the last resort. *Aspergillus* fungal wall galactomannan, a useful biomarker, which is measured in blood (which has a sensitivity of 79–96% and specificity 74–99%) or BAL fluid (which has a sensitivity 67–100% and specificity of 78–100%).

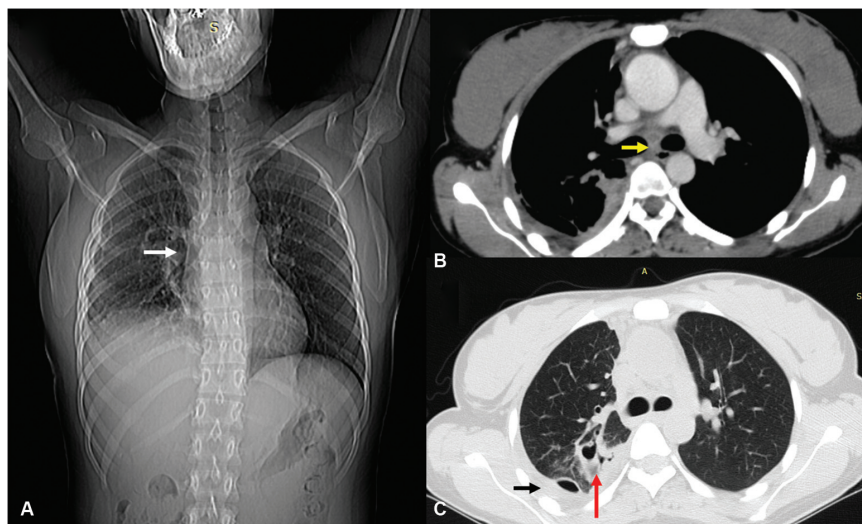


Fig. 9 (A–C) Thoracic imaging studies of a 22-year-old female, a known case human immunodeficiency virus, with cough, fever, and chest pain, CD-4, 400/ μ L. Chest radiograph shows right hilar lymph adenopathy (white arrow) and right pleural effusion. Contrast-enhanced computed tomography, mediastinal window (B), shows carinal lymph adenopathy (yellow arrow). Lung windows (C) show cavitating consolidation in superior segment of the right lower lobe (red arrow) with right pleural effusion (black arrow). All features are characteristic of tuberculosis and sputum smear examination confirmed the same.

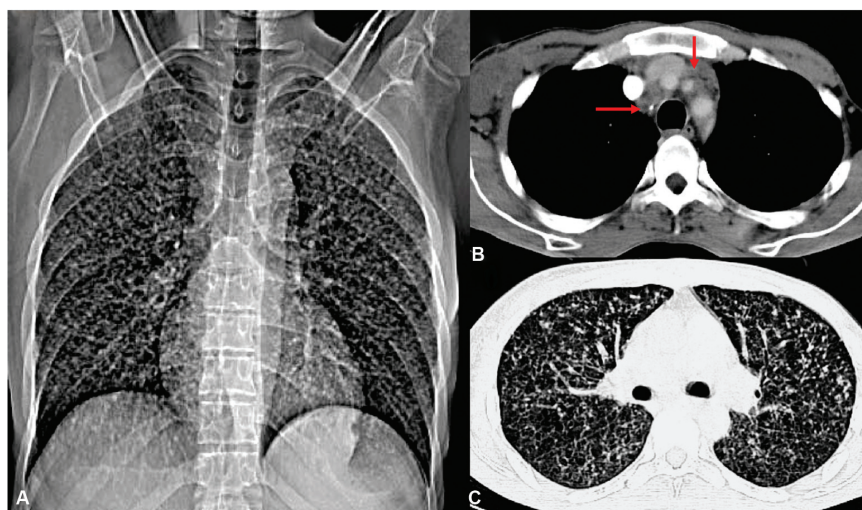


Fig. 10 (A–C) Contrast-enhanced computed tomography (CECT) a 35-year-old male, a known case of human immunodeficiency virus, with sudden onset cough, fever, and respiratory distress with a CD-4 <200/ μ L. Scout view shows bilateral multiple micronodular (miliary) opacities. CECT, mediastinal window (B) show nonenhancing, paratracheal lymph nodes (red arrow). Lung window (C) shows bilateral miliary opacities, no interstitial abnormality. Features are characteristic of tuberculosis; diagnosis was confirmed by transbronchial lung biopsy and presence of epithelioid cells in bronchoalveolar lavage fluid. Sputum is usually negative in miliary tuberculosis.

Treatment: Voriconazole is commonly used to treat these fungal infections. Other agents include amphotericin, posaconazole, isavuconazole, and echinocandins.⁵⁸

***Pneumocystis jirovecii* (PJP) (previously known as *Pneumocystis carinii* pneumonia or PCP)**

Clinical setting and features: The infection occurs in patients with a severe immune deficiency, such as renal transplant, hematopoietic stem cell transplant, and HIV patients. According to most reports, *P. jirovecii* is the second most common infection after tuberculosis in HIV-afflicted patients. The clinical symptoms are insidious

onset fever, dry cough, and worsening dyspnea, which persist for about a month prior to presentation. Patients are usually hypoxic at the time of presentation.^{4,15,45,46,59,60}

Imaging: The radiographs and CT show a GGO pattern, which may be interspersed with a reticulonodular pattern that is initially parahilar and later becomes more diffuse in distribution. HRCT in the early phase typically reveals large areas of GGOs with a relative sparing of peripheral areas and upper lobes. There is a stark contrast between the partially opacified lung and the air filled bronchus, which is seen as a “**dark bronchus**” sign. The latter sign is useful especially if the GGOs are subtle. With progression, the involved areas with GGO become more

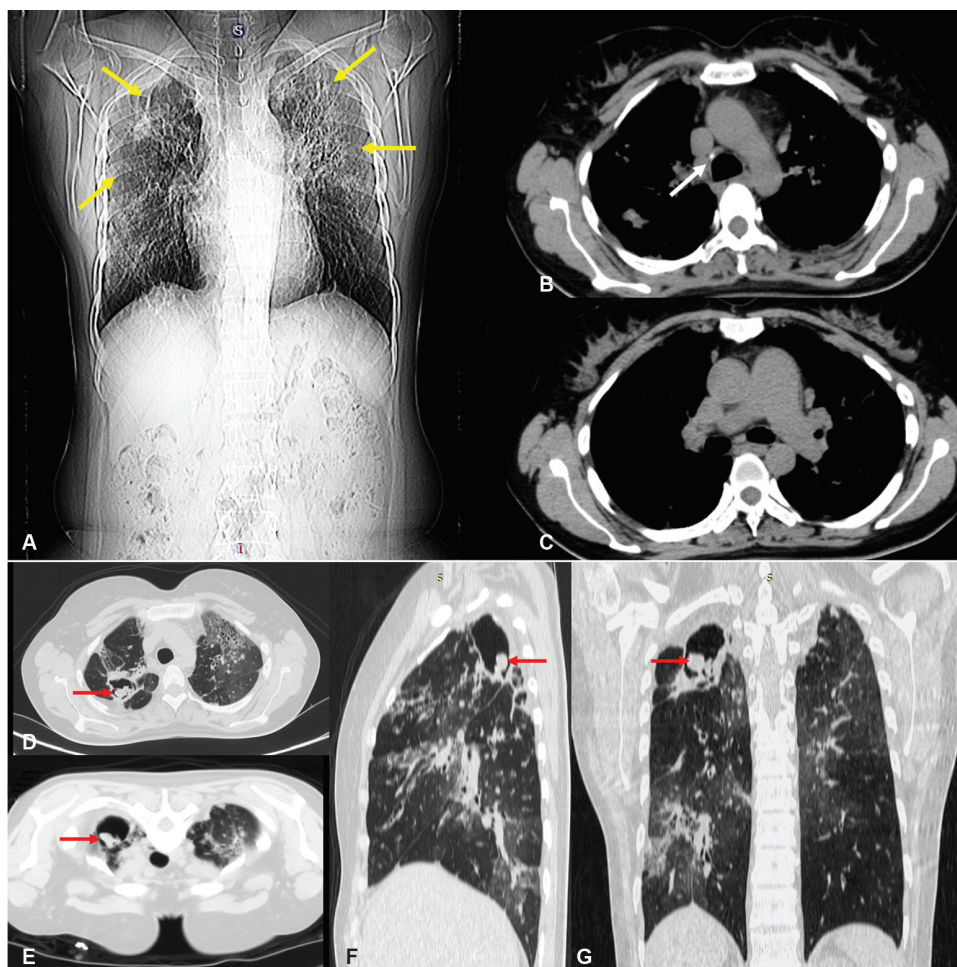


Fig. 11 Imaging studies of a 35-year-old female, a known case human immunodeficiency virus, on treatment for tuberculosis, complaining of recent hemoptysis. Chest radiograph (A) shows bilateral upper and mid-zone infiltrates (yellow arrows). Computed tomography, mediastinal windows, shows calcified pretracheal lymph nodes (white arrow) (B, C). Lung windows (D–G) show a mobile soft tissue mass (red arrows) within a right upper lobe cavity (D, supine) and (E, prone). Features are characteristic of aspergilloma in a preexisting lung cavity (in this case due to tuberculosis). The suspected fungus confirmed on sputum examination.

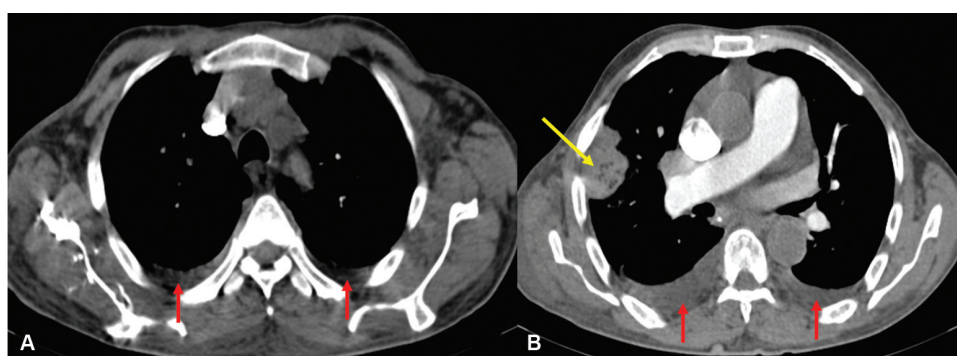


Fig. 12 (A, B) Contrast-enhanced computed tomography (CECT) thorax a 65-year-old male, diabetic, chronic alcoholic, chest pain, and low-grade fever for the last 1 month. Scout view had shown subpleural mass in right mid-zone. CECT mediastinal windows shows a pleural based mass in right upper lobe (yellow arrow). The mass was poorly enhancing. Right pleural effusion is also present (red arrows). The appearances are characteristic for chronic abscess in chest wall, most likely fungal origin. Examination of the fluid obtained by ultrasound-guided aspirate revealed *Aspergillus fumigatus*.

diffuse and characteristically show variable-sized peripheral and central cysts in up to 30% of patients. Rupture of cysts is likely, and manifests as pneumothorax and/or pneumomediastinum (►Fig. 17).^{4,15,45,46,59–62} The etiology of cysts has been

proposed as over distension of airspaces by obstructive bronchiolitis through a ball valve mechanism. With advanced disease, septal lines and intralobular lines superimpose on GGO, resulting in “crazy paving” appearance (►Fig. 18). Some areas

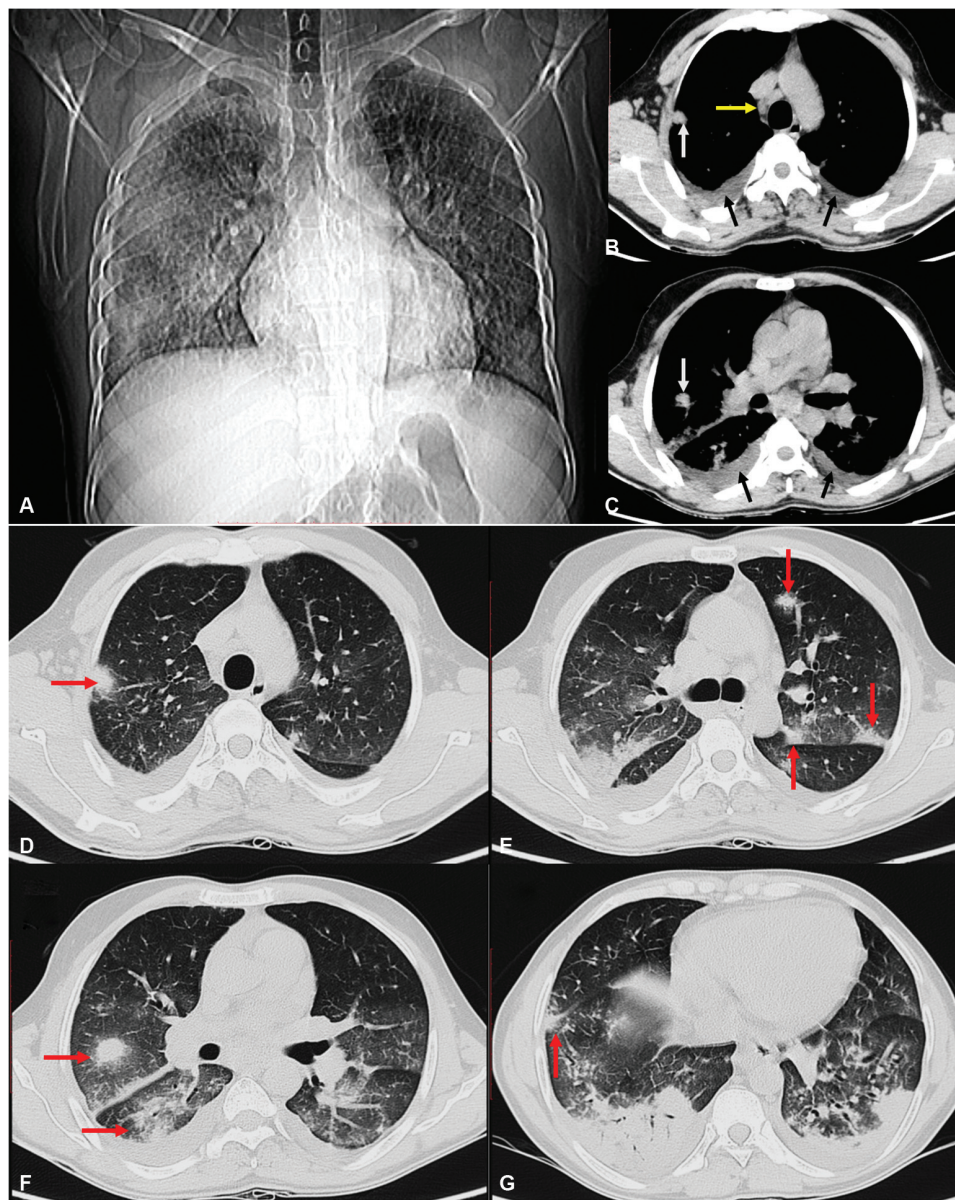


Fig. 13 Contrast-enhanced computed tomography of febrile neutropenia in a 48-year-old male, with hematological malignancy. Scout view (A) shows bilateral ground glass opacification and nodules. Mediastinal window (B, C) shows paratracheal lymph nodes (yellow arrow), peripheral nodules (white arrows) in right lung and bilateral pleural effusion (black arrows). Lung windows (D–G) show subsegmental consolidation both lungs and multiple nodules, some with spiculated margins, all with ground glass halo (red arrows). The diagnosis of angioinvasive aspergillosis was confirmed by serology and examination of bronchoalveolar lavage fluid.

may even progress to subsegmental and segmental consolidation, with air bronchogram (►Fig. 19). Pleural involvement initially begins with minimal effusion, but in patients with cysts, multiple pockets of pneumothorax are seen. These may resolve spontaneously or with treatment. Recovery may leave behind interstitial fibrosis. Atypical presentations also include a primary presentation as an acute interstitial pneumonitis. An unusual association with an intracranial lesion (abscess) has also been described, which was documented in one of our patients (►Fig. 19 is of the said patient who also had an associated intracranial abscess) (intracranial lesion image not shown).^{15,45,61–63}

Differential diagnosis to be considered for the imaging pattern includes CMV pneumonia, which, however, has more of nodular pattern and a basal predilection, while parahilar predominance and the presence of cysts are more in favor of *P. jirovecii* infection. The GGOs may simulate angioinvasive fungal disease, but the presence of “halo” sign, “reverse-halo” sign, and “air-crescent” sign, all definitely distinguish angioinvasive aspergillosis infection from *P. jirovecii*. Other causes of isolated GGOs may be an alveolar form of pulmonary edema and diffuse alveolar hemorrhage (a sequelae of acute lung injury, especially in hematopoietic stem cell transplant patients).¹⁵

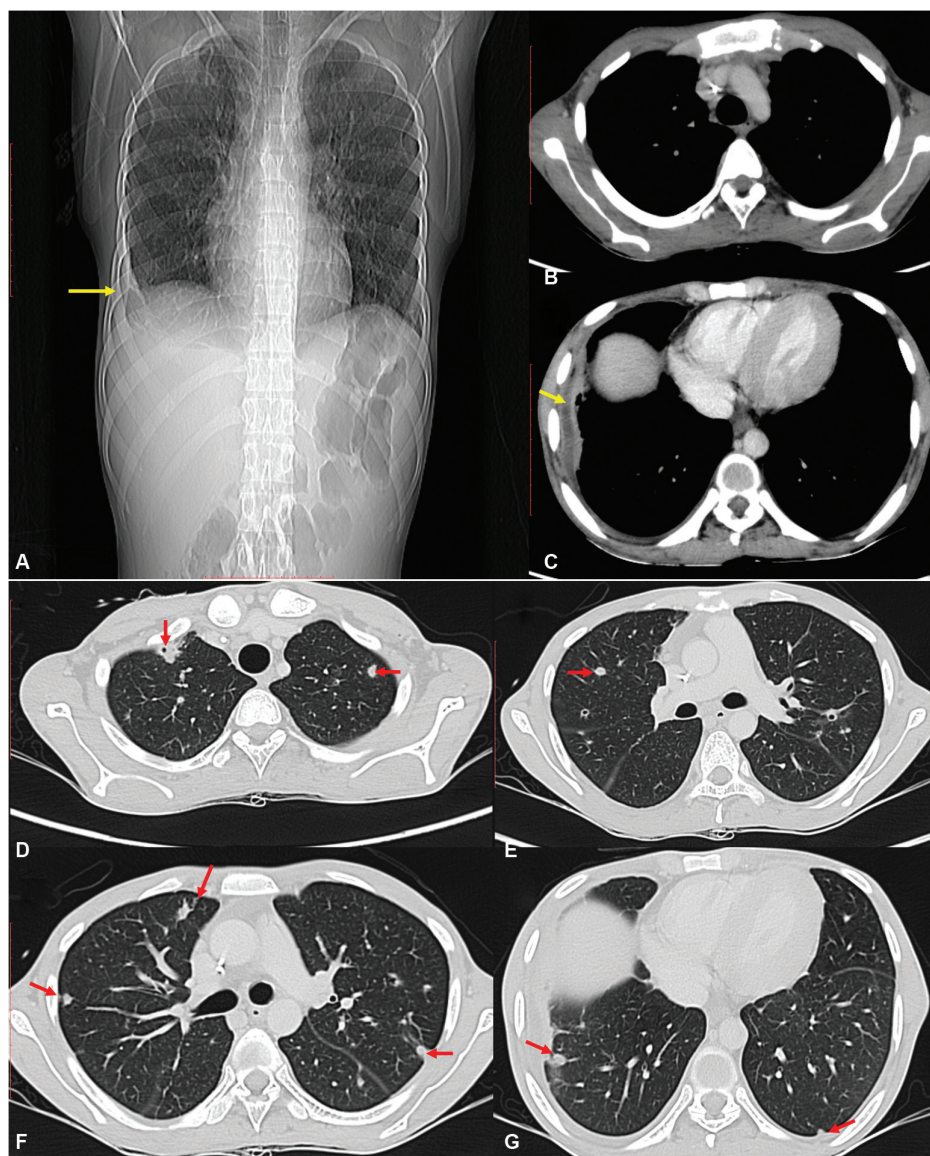


Fig. 14 Contrast-enhanced computed tomography for febrile neutropenia in a 30-year-old male with hematological malignancy. Scout view (A) and mediastinal window (B, C) show right pleural effusion (yellow arrows). Lung windows (D–G) show bilateral, multiple subpleural nodules with “ground glass halo” (red arrows), and loculated right pleural fluid (yellow arrow)(C). The diagnosis of angioinvasive aspergillosis was confirmed by serology and examination of bronchoalveolar lavage (BAL) fluid.

The diagnosis is confirmed by microscopic examination of BAL fluid, lung biopsy, or induced sputum. The cell wall is stained by GMS stain, which clearly demonstrates the trophic and cystic forms of the fungus. Polymerase chain reaction of BAL fluid is an emerging technique for the diagnosis of this fungal organism.

Treatment: A Trimethoprim–sulfamethoxazole combination is the preferred treatment. Those patients with an A-a (alveolar–arterial) gradient of greater than 36 mm Hg benefit from steroids. A prophylaxis with co-trimoxazole is recommended and administered for those with a CD-4 count less than 200 cells/ μ L.^{45,46,59,61–63}

Histoplasmosis

Clinical setting: In the authors experience, histoplasmosis is not as common as *Aspergillus* and *Candida* infection in

immunocompromised hosts, but should be considered if the patient hails from the endemic areas along the Gangetic plains of India. In the Americas, it occurs in North, Central, and South America. The fungi inhabit geographical regions rich in bird or bat droppings. **We have found it more common in patients who are diabetic and male. Patients who are HIV infected are prone to have histoplasmosis** as an opportunistic infection and is also considered an **AIDS-defining illness**. The onset is subacute, with worsening fever, cough, dyspnea, and heaviness in chest. **The important clinical clues to the infection by this fungus are the presence of oral ulcers and cutaneous lesions.** Most patients have a multiorgan disseminated disease, by the time they seek medical attention. The clinical presentation has been rightly called by Gopalakrishnan et al, as “**sub-acute progressive disseminated.**” The organism typically

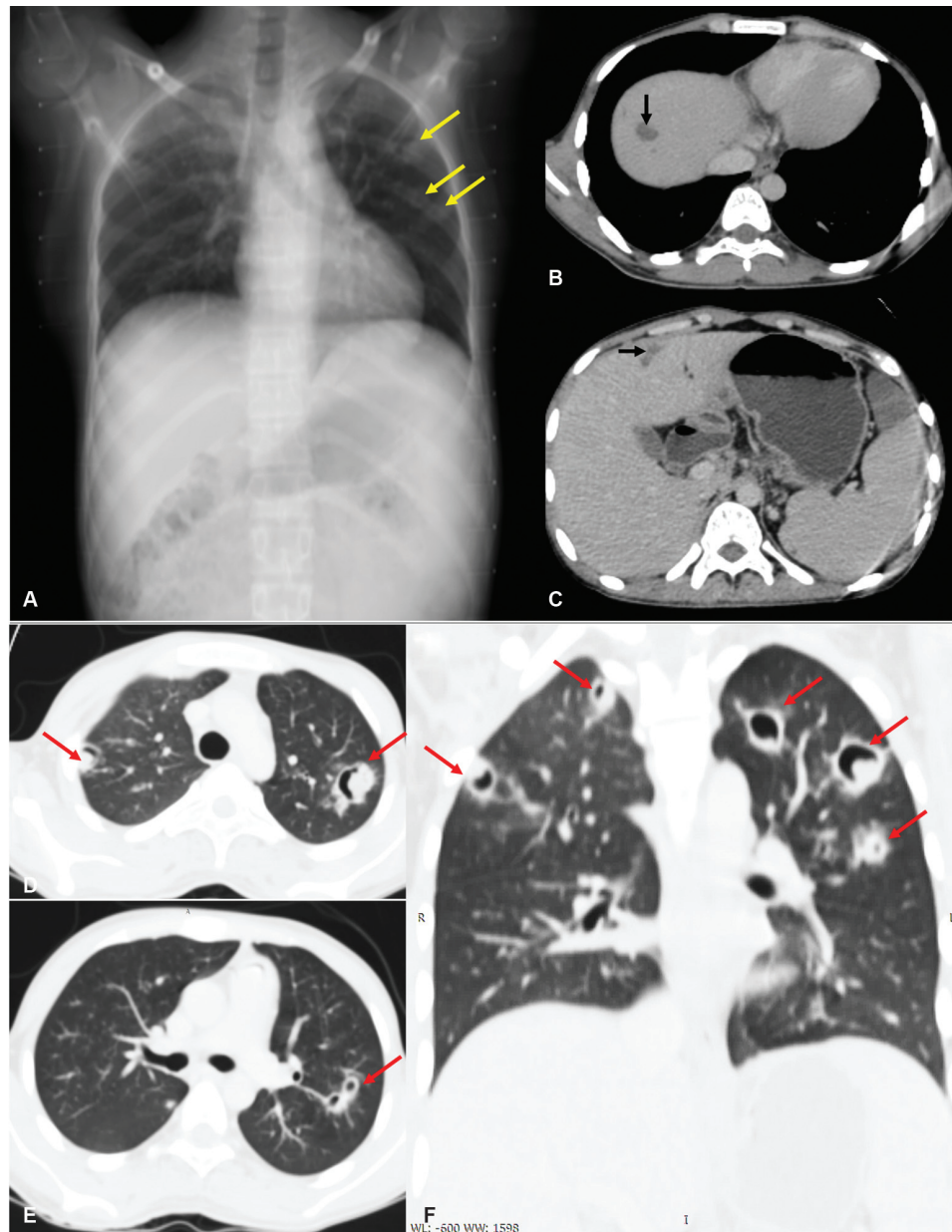


Fig. 15 Thoracic imaging for febrile neutropenia in a 28-year-old male, with hematological malignancy. Chest radiograph (A) shows left upper and mid-zone nodular shadows (yellow arrows). Contrast-enhanced computed tomography mediastinal window (B, C) shows hypodense lesions in right lobe of liver (black arrows). Lung windows (D–F) show bilateral, multiple subpleural nodules with air crescent sign (red arrows), indicating (recovery phase of) angioinvasive aspergillosis. Hepatic involvement is noteworthy. The diagnosis was confirmed by serology and examination of bronchoalveolar lavage (BAL) fluid.

invades adrenal glands and causes adrenomegaly, besides hepato-splenomegaly and mediastinal and abdominal lymphadenopathy. Occasionally, signs and symptoms of adrenal insufficiency such as dizziness, fatigue, and sweating due to hypotension and hypoglycemia are present.^{38,42,44,64}

Radiological and imaging features in the lung simulate tuberculosis to a great extent with the presence of mediastinal lymphadenopathy and bilateral lung lesions. The lung lesions show a mixed pattern with **fibrosis, nodules, patchy consolidation, and cavitation all present together** (→ Fig. 20). Isolated reports describe miliary dissemination, like in tuberculosis and subpleural nodules like in metastatic malignancy. **Fibrosing mediastinitis compressing the ma-**

ajor vessels, if present, is considered a characteristic sign. Pleural involvement does not occur. The clinical features of hepatomegaly and hypoadrenalism are leading clues to extend the CT study for evaluation of the abdomen. **The adrenals typically show bilateral, but asymmetrical involvement with enlargement, showing peripheral enhancement and central hypoattenuation due to necrosis** (→ Fig. 20). **Co-existing adrenal involvement and mucocutaneous lesions are important indicators for the aetiology of Histoplasma infection and their simultaneous occurrence also affect the patient prognosis.**^{38,39,42,43,64}

Differential diagnosis: The most frequently overlapping imaging diagnosis is tuberculosis, if the images are evaluated

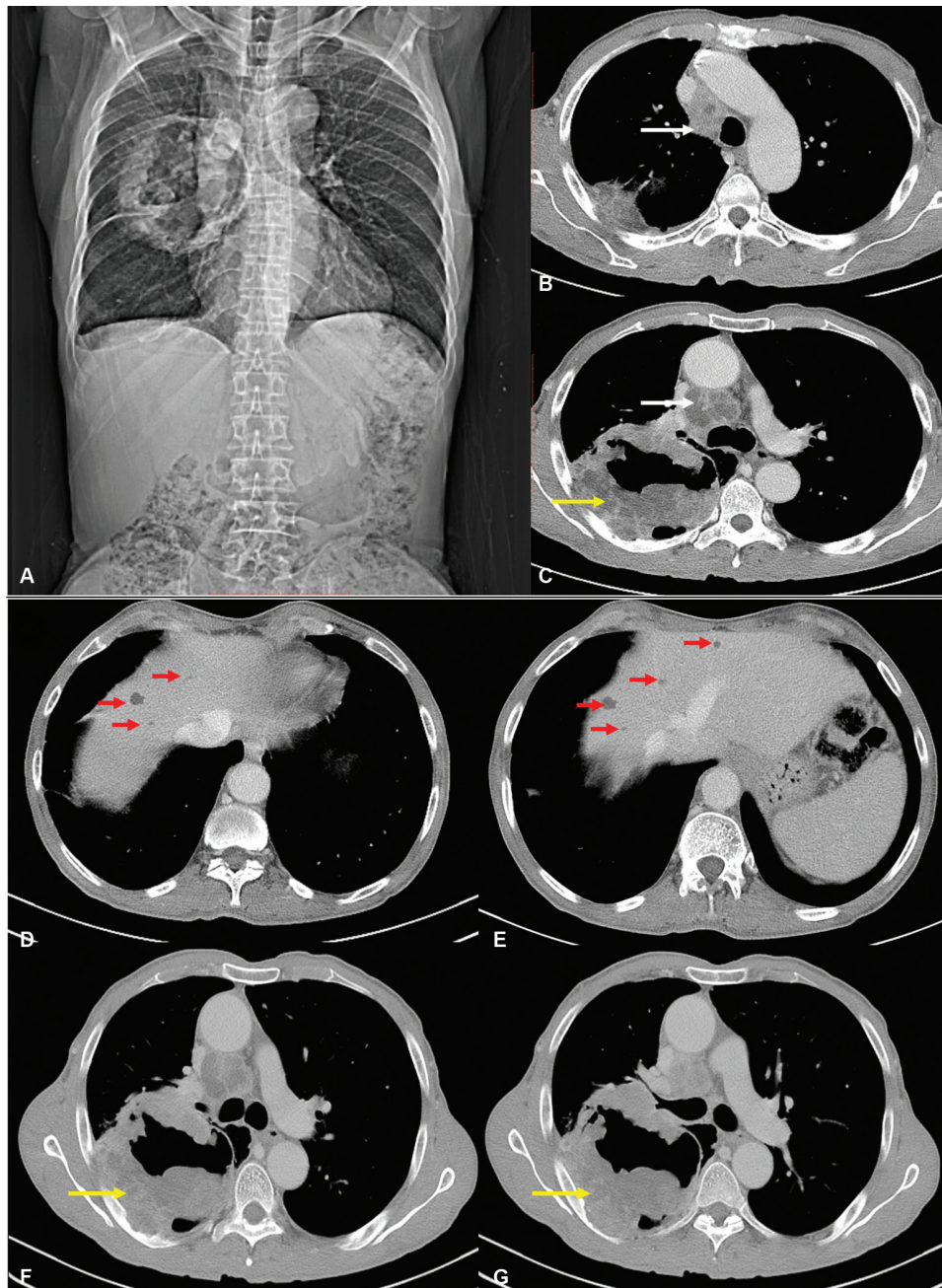


Fig. 16 Thoracic imaging for cough, hemoptysis, pyrexia in a 45-year-old male, with hematological malignancy. The chest radiograph (A) shows large thick-walled cavity, in the right mid-zone. Contrast-enhanced computed tomography mediastinal window (B–G) shows rim enhancing subcarinal node, large thick-walled cavity in right upper lobe (yellow arrows), multiple microabscesses in right lobe of liver (red arrows). Lung windows (H–K) show a spherical region of consolidation, with central necrosis, forming a large thick walled cavity with a central mass (yellow arrows). A diagnosis of disseminated fungal infection was considered and *Candida* was confirmed.

without due diligence. **The radiological features that favor histoplasmosis are the absence of significant pleural effusion, presence of subpleural nodule/s, fibrosing mediastinitis, associated hepatosplenomegaly without focal lesions, and necrotic adrenomegaly.**^{38,39,42–44,64} Tuberculosis always has focal macronodular or miliary (micronodular) hepatosplenic involvement, along with which adrenal involvement may be present.

The diagnosis is confirmed by fungal culture of BAL fluid and transbronchial biopsy specimens. Urinary and BAL anti-

gen test for histoplasma and tissue histopathology showing budding yeast 2 to 4 μ m in diameter are conclusive diagnostic tests.

Treatment: Amphotericin B and itraconazole are used for treatment.^{38,39,42–44,64}

Mucormycosis

Clinical setting: Mucormycosis (older nomenclature: zygomycosis) is caused by a **group of fungi of the Mucorales family, which characteristically causes simultaneous**

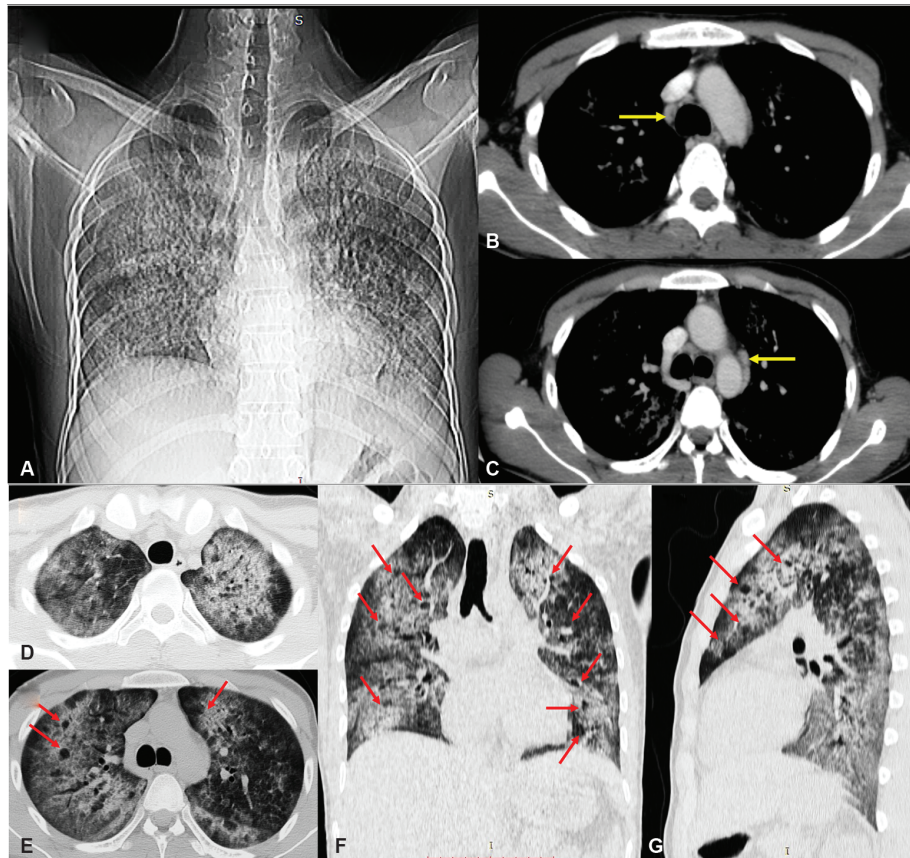


Fig. 17 (A–G) Thoracic imaging in a 25-year-old male with human immunodeficiency virus, high grade fever, respiratory distress, and CD-4 counts $40/\mu\text{L}$. Scout view shows bilateral diffuse ground glass and reticulonodular opacities. Mediastinal windows (B, C) show pre- and paratracheal lymph nodes (yellow arrows). Lung windows (D–G) show bilateral diffuse ground glass and reticular opacities with multiple areas of cyst formation (red arrows). The appearances are characteristic for *Pneumocystis jirovecii* infection. The organism was isolated from induced sputum and bronchoalveolar lavage washing.

invasion of rhino-cerebral, orbital, pulmonary, and gastrointestinal structures and is rapidly fatal if left untreated. Conversely, early treatment significantly improves the chances of survival.⁶⁵ The patients prone to infection by mucormycosis include those with **uncontrolled diabetes, hematological malignancy (especially those with acute leukemia), stem cell transplant, solid organ transplant, neutropenia, and steroid use.** It is known that lung infection is more common in solid organ transplant patients, whereas rhinocerebral infection is more likely in patients with uncontrolled diabetes mellitus. The clinical presentation is subacute with cough, dyspnea, and fever for about 2 to 4 weeks, followed by hemoptysis in a few cases.^{65–67} An increased incidence of paranasal mucormycosis with orbital invasion has been observed by us in patients who have received high-dose steroids during a moderate or severe infection or recovery phase of COVID-19 pneumonitis, which has now been reported by various other Investigators as well.

Radiological and imaging features of pulmonary infection: The picture is a nonspecific one and few features resemble those of angioinvasive candidiasis/aspergillosis, as the early stages may show a single or a few ground-glass nodules. However, the lesions in mucormycosis are more often in upper lobes and also more often peripherally located

(**Fig. 21**). The condition rapidly progresses to a mixed one, with multiple nodules intermixed with patches of consolidation. The consolidation patches may surround a central GGO, thus fulfilling the criteria for a reverse halo sign. **The reverse halo sign is most frequently observed in mucormycosis, compared with all other fungal infections. Air bronchograms are conspicuous by their absence, even in dense consolidation.** Cavitation may occur rapidly in the patches of consolidation, probably due to vascular compromise. **Vascular compromise being frequent in this infection, pulmonary vascular cut off and/or emboli manifesting as vascular filling defects are often seen.** In a few patients, an invasion of the chest wall, diaphragm, and mediastinum may be seen. **Coexisting clinical and/or radiological rhinocerebral involvement is an important clue to the diagnosis of mucormycosis and disseminated disease also affects the patient prognosis** (**Fig. 21**). The active role of the radiologist is to consider the possibility of mucormycosis, by obtaining brain, orbit, and paranasal sinus imaging in the same sitting, when the patient is sent for a pulmonary imaging evaluation.^{65–67}

Differential diagnosis: The mixed picture of GGOs, nodules, consolidation, reverse halo sign, and pulmonary emboli may simulate candidiasis, aspergillosis, and histoplasmosis. However, the subacute clinical presentation, peripheral

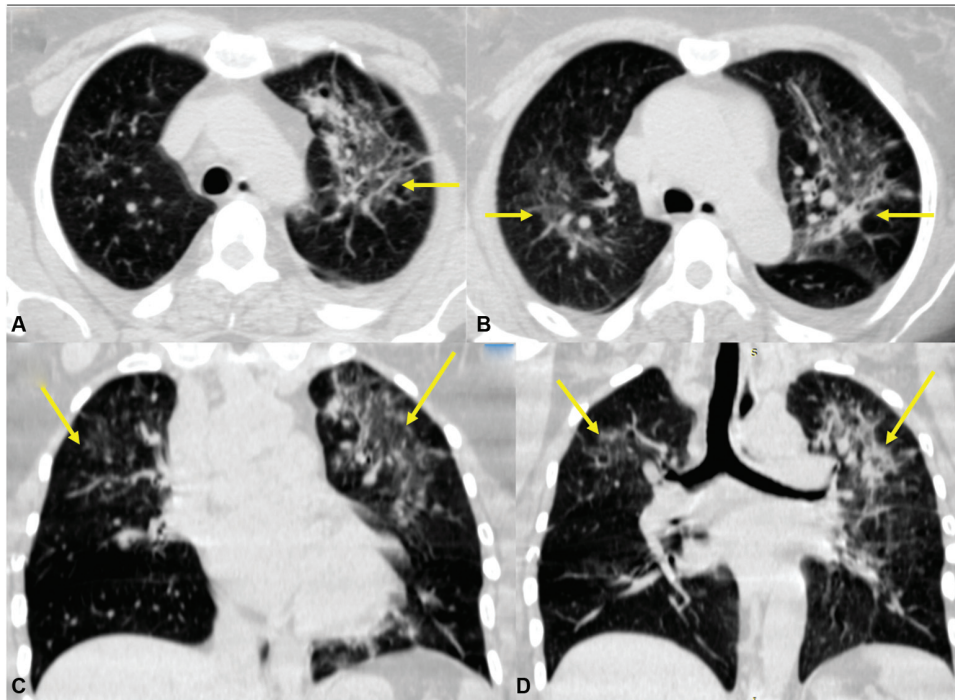


Fig. 18 Thoracic imaging in a 46-year-old male with chronic kidney disease, complaints of high-grade fever, respiratory distress, and seizure. Computed tomography of the brain had shown a focal enhancing lesion. Lung windows (A–D) of the thoracic study show bilateral multiple ground glass and reticular opacities (yellow arrows) with areas of cyst formation. The appearances are characteristic for *Pneumocystis jirovecii* infection. The organism was isolated from bronchoalveolar lavage washing (associated intracranial lesions are rare).

location of lesions, more of reverse-halo signs, absence of air bronchogram, features of pulmonary vascular compromise, and coexisting rhinocerebral and orbital involvement are all important clues to the etiology of mucormycosis.^{65–67}

The diagnosis is confirmed by either transbronchial or percutaneous lung biopsy, using Calcofluor white or Blankophor optical brighteners for staining and also by a fungal culture.^{65,66} **Treatment** includes expeditious eradication of risk factors, commencement of anti-Mucor therapy, and surgical resection, as the condition has a high mortality. Liposomal amphotericin B is the commonest drug used for the first-line treatment, and posaconazole for first-line as well as salvage treatment. Surgical resection in addition to antifungal therapy is a common recourse.^{65,66}

Cryptococcal pneumonia: Infections with *Cryptococcus* occur worldwide, in severe immunosuppression especially in AIDS patients, when the CD-4 counts fall below 100 cells/mm³. **Cryptococcus should be considered as the offending agent in AIDS patients when laboratory tests for tuberculosis and *P. jirovecii* are negative.** The primary route of infection is the lung, which then leads to disseminated disease, with a great propensity for central nervous system (CNS) involvement in the form of meningoencephalitis. The lung CT pattern shows various types of **peripherally located lesions: either only nodular masses or only pneumonic infiltrates, or GGOs or a mixed one.** Mediastinal lymph node enlargement and pleural effusion are known. **Associated CNS involvement is characteristic of this disease and will affect the patient treatment and prognosis.**⁶⁷

The diagnosis is confirmed either by a serum agglutination test or by transbronchial/CT-guided percutaneous biopsy of lung followed by fungal culture of respiratory fluids.⁶⁷

The principles of management of cryptococcal infection include (1) induction therapy for meningoencephalitis using fungicidal regimens, such as a polyene and flucytosine, followed by suppressive regimens using fluconazole; (2) early recognition and treatment of increased intracranial pressure and/or immune reconstitution inflammatory syndrome; and (3) the use of lipid formulations of amphotericin B regimens in patients with renal impairment.^{67,68}

Blastomycosis is endemic mainly to North America, although isolated cases have been reported from Africa and India. **The imaging features on CT** are similar to *Cryptococcus*, with a mixed pattern of interstitial and parenchymal lesions. The parenchymal lesions can be **mixed, with GGOs, tree-in-bud opacities, patchy consolidation all present together, or even simulate a malignancy,** especially when a parahilar mass is present. Mediastinal lymphadenopathy, pleural effusion, nonresolving consolidation, and calcified granulomas have also been reported. **Associated skin lesions are important clues to the diagnosis as in histoplasmosis.**^{48,69}

The differential diagnosis from other fungal infections and tuberculosis may be difficult, when only imaging studies are evaluated in isolation. However, blastomycosis should be considered in patients with skin lesions and laboratory tests negative for tuberculosis and aspergillosis and also if the patient hails from or has visited an endemic area.

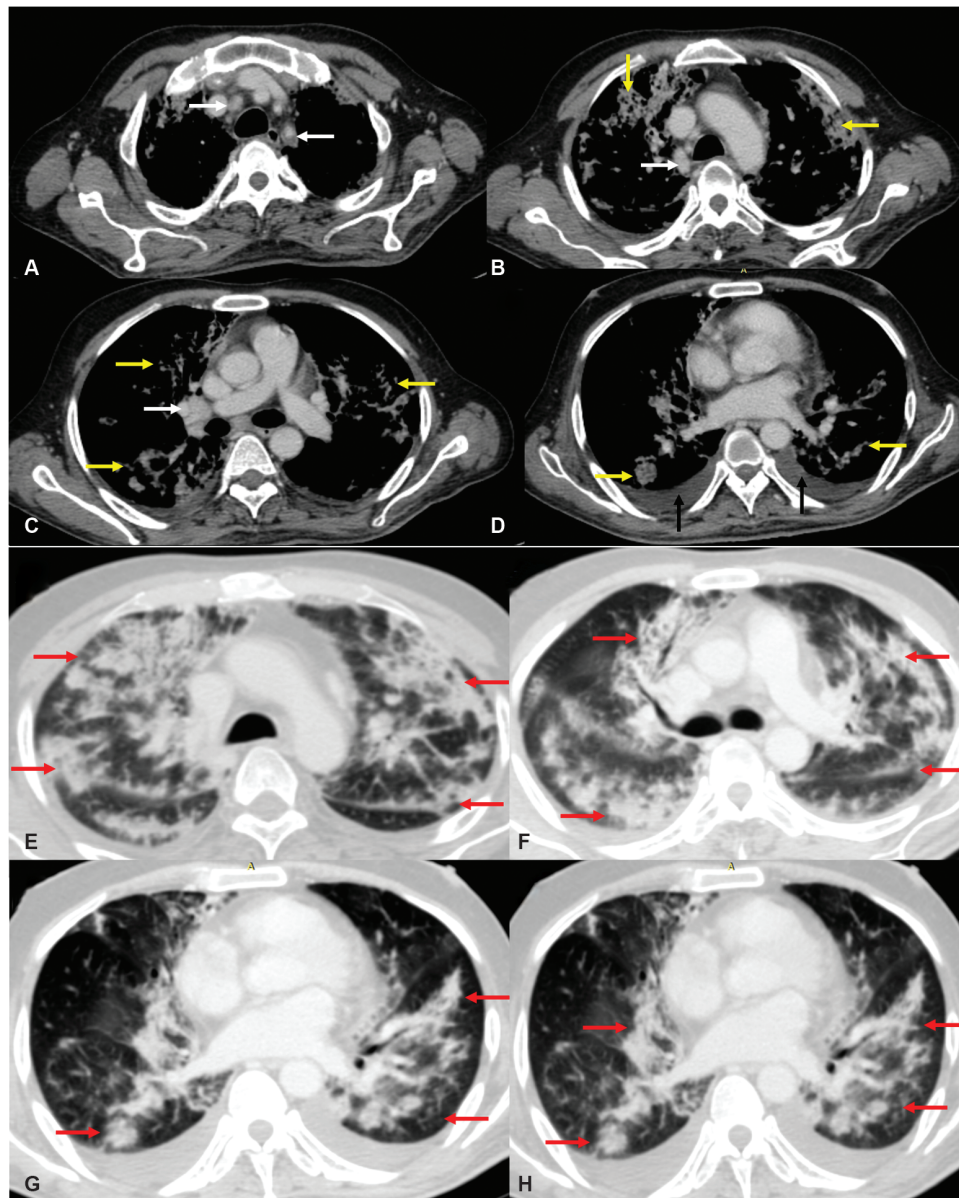


Fig. 19 Thoracic imaging of a 52-year-old male with human immunodeficiency virus, complaints of high-grade fever, respiratory distress, CD-4 count $20/\mu\text{L}$. Mediastinal windows (A–D) show pre- and paratracheal lymph nodes (white arrows) with nodular opacities and patchy consolidation (yellow arrows). Bilateral pleural effusion present (black arrows). Lung windows (E–H) show bilateral diffuse ground glass opacities that are coalescing, interspersed reticular opacities, and multiple cysts (red arrows). The appearances are characteristic for *Pneumocystis jirovecii* infection. The organism was isolated from induced sputum and bronchoalveolar lavage fluid as well.

The diagnosis is confirmed by transbronchial or CT-guided lung biopsy and fungal culture from BAL fluid. In a few reported cases, the condition has come to light only at surgical resection for a suspected malignancy.^{48,69}

Treatment: Itraconazole is typically used to treat mild-to-moderate blastomycosis, while amphotericin B is usually recommended for severe pulmonary blastomycosis.^{48,69}

Viral Infections

Cytomegalovirus (CMV) infection

Most common viral infection among the immunocompromised patients are CMV, VZV, HSV, respiratory syncytial virus, parainfluenza virus, and influenza virus. The risk

factors for viral pneumonia and bacterial pneumonia are almost similar and both may coexist. However, the most significant viral pulmonary infection in terms of morbidity and mortality in immunocompromised patients occurs with CMV infection, which typically occurs in solid organ transplant and bone marrow transplant patients. The CMV is a DNA virus of the *Herpesviridae* family, which also includes VZV, HSV 1 and 2, and the Ebola virus. This infection is most likely in severe immune suppression, when CD-4 counts are below $100\text{ cells}/\mu\text{L}$. Early suspicion and recognition of CMV infection are clinically significant, especially in solid organ transplant patients, as it is an important cause of transplant rejection, due to secretion of cytokines and growth factors.^{12,13,15,70–73}

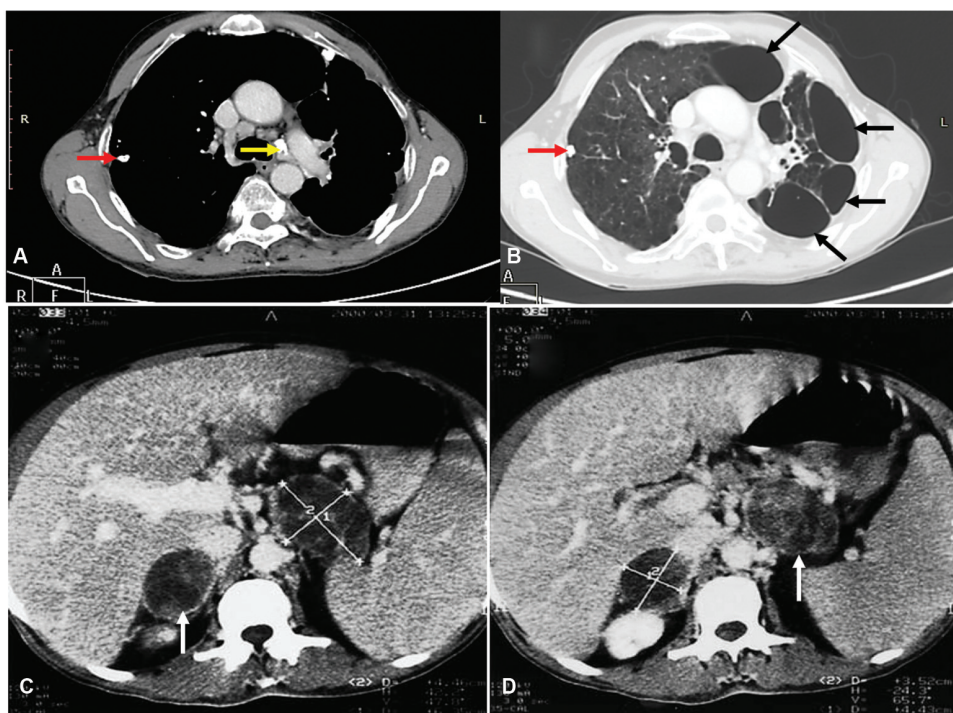


Fig. 20 Thoracic, upper abdomen computed tomography (CT) of a 54-year-old male, diabetic, with complaints of cough, dyspnea, and low-grade fever for the last 5 weeks. Thoracic CT study, mediastinal window (A) shows paratracheal lymph nodes, some with dense calcification (yellow arrow), along with calcified subpleural nodule in right lung (red arrow). Lung window (B) shows multiple bronchiectatic and fibrocavitary lesions in left upper lobe (black arrow). Upper abdomen sections (C, D) show that both adrenals are enlarged and hypodense (white arrows). The appearances suggested tuberculosis; CT-guided aspirate revealed histoplasmosis. (Reproduced with permission of copyright holders).³⁸

Clinical Setting

The infection is more likely in posttransplant patients in the early posttransplant period between 31 and 100 days. The infection is considered to be of a primary type, either by receiving a CMV positive donor transplant or a secondary type due to reactivation of a latent infection.^{12,13,15,70-72}

Imaging features: Radiograph and CT reflect pathologies of bronchiolitis and parenchymal disease. **Initially, bilateral parahilar, GGO, and a few nodules with halo are seen, which may later coalesce to form subsegmental or lobar consolidation** (► Fig. 22). The nodules are peribronchial in location. Bronchiolitis results in hypoventilation of alveoli distal to the bronchiolar obstruction, subsequent to which these areas are under perfused and hypoattenuating, resulting in a **“mosaic pattern” or a reduction in lung attenuation. Mosaic attenuation is best confirmed on expiratory CT or radiographs.** The presence of peribronchial and septal thickening super-imposed on ground-glass opacification is characteristic and is known as **“crazy paving” appearance** (► Fig. 22). Bilateral pleural effusion occurs in up to 60% cases.^{12,13,15,70-72}

Differential diagnosis: Most viral infections show mixed alveolar and bronchiolar involvement and a specific diagnosis among the different viruses is often not possible by imaging alone. The mixed reticulonodular with parenchymal opacification pattern occurring together and appearing as “crazy paving” is an important clue to suspect a virus as the infective agent. Fungal infections may also show reticulonodular pattern, and GGOs, but diffuse GGOs with crazy

paving, largely in parahilar location, are more in favor of CMV pneumonia. Moreover, fungal infections additionally have micro- and macronodules.

The diagnosis is confirmed by CMV antigen assay and/or TBLB.^{12,13,15,70-72} **Treatment** is by combination of ganciclovir, valganciclovir, and foscarnet.⁷³

COVID-19 Infection

Clinical setting: COVID-19 infection or coronavirus disease is due to the novel coronavirus, named nCoV-2019, which originated in Wuhan, China, in December, 2019 and subsequently erupted into a global pandemic. The virus has been found to invade respiratory epithelial cells through an interaction between viral protein and angiotensin-converting enzyme 2 receptor on these cells and subsequently affect other organs. This viral infection typically begins as a pyrexia with mild respiratory infection, which usually resolves uneventfully within a few weeks in young adults. However, in mildly immunocompromised individuals, such as the elderly or patients with diabetes, hypertension, and cardiac disease, the condition rapidly deteriorates into a pneumonia with respiratory distress and acute respiratory failure. **Paradoxically however, when AIDS patients on HAART are infected with COVID-19, they show earlier and more complete recovery on treatment with COVID-19 specific antiviral agents, compared with immunocompetent patients.**⁷⁴⁻⁷⁶

Radiological and imaging evaluation is recommended for early diagnosis, assessment of severity, and for post-treatment surveillance. Early diagnosis not only allows for

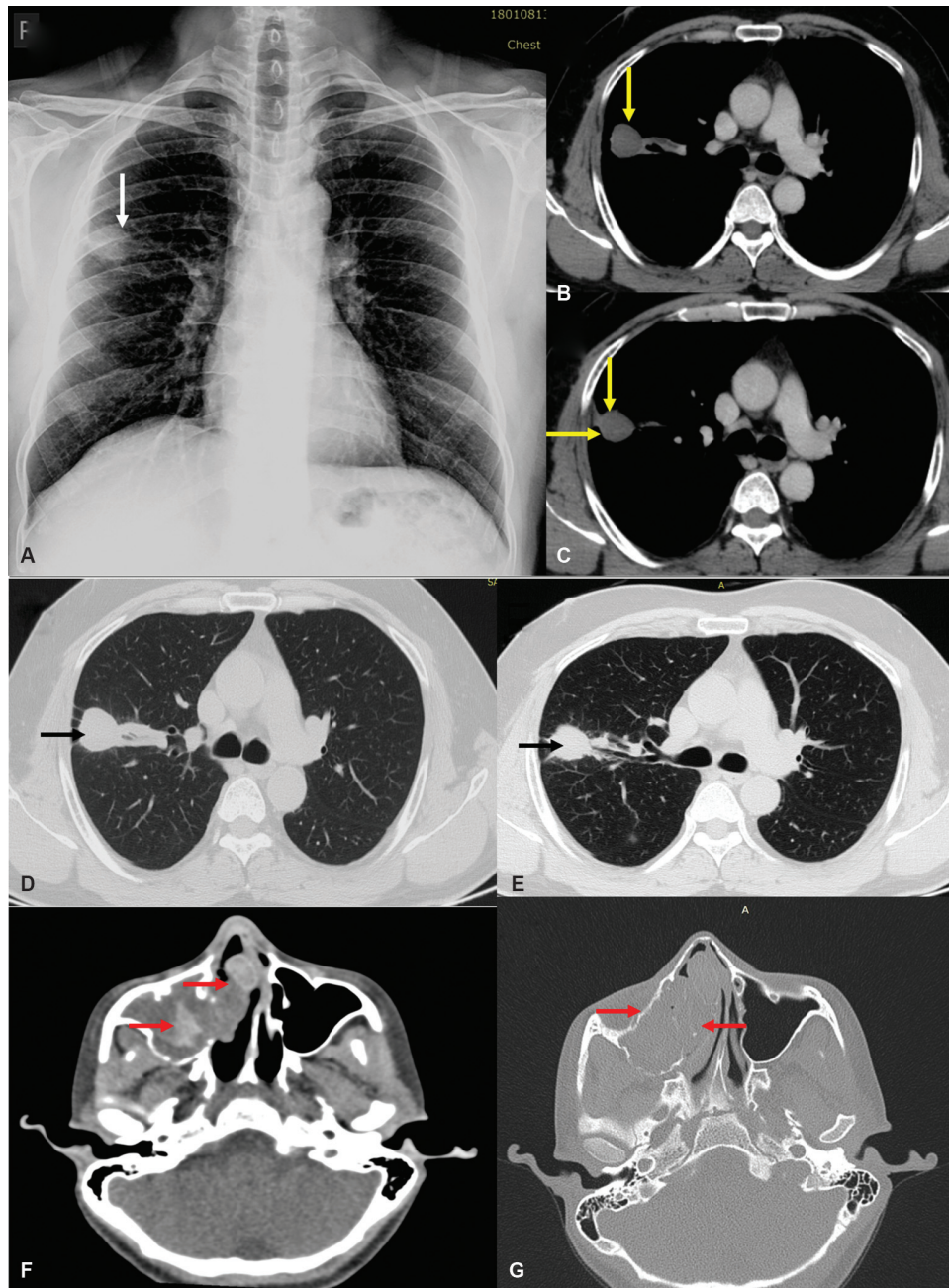


Fig. 21 Thoracic, paranasal sinus contrast-enhanced computed tomography (CECT) of 32-year-old male, with uncontrolled diabetes, cough, fever, pleuritic pain, for the last 2 weeks. Chest radiograph (A) shows peripherally located opacity, right mid-zone (white arrow). CECT mediastinal window (B, C) shows pre- and paratracheal lymph nodes and a subpleural macro nodule in the right lung (yellow arrows). Lung windows (D, E) show bronchiectatic traction toward spiculated mass in right middle lobe (black arrow). Paranasal sinuses (F, G) show hyperdense masses and bone erosion (red arrows). The imaging appearances were characteristic for Mucormycosis, which was confirmed a CT guided aspirate from the subpleural nodule.

early institution of treatment but also immediate isolation to contain further person-to-person spread. A chest radiograph and HRCT are recommended. The CO-RADS image reporting and data system has been devised to standardize the prediction of COVID 19 infection based on CT Scans alone. The Semiquantitative CT Severity Score, CTSS, on the other hand, has been devised to assign severity of lung involvement and has been found to correlate well with clinical severity. Imaging studies may be negative in the first 1 to 2 days of illness in up to 50% of cases; however,

abnormalities invariably appear within the first 3 to 7 days (intermediate stage of illness) or in the second week (late phase of illness). The characteristic features are **bilateral subsegmental, peripherally located, subpleural, ill-defined areas of GGO, more often in lower lobes**. Some of the GGOs may have a reverse halo sign. These opacities are may sometimes be accompanied by irregular interlobular septal thickening, giving rise to “crazy paving” (►Fig. 23). The condition subsequently progresses to complete opacification and later to consolidation with air bronchogram,

and thickening of adjoining pleura. Nodular lesions, pleural effusion, and lymphadenopathy are usually absent. CTPA may be done if the clinical scenario suggests pulmonary embolism. With adequate and timely medical support, majority of patients show complete clinical and imaging recovery in the third to fourth week.⁷⁴⁻⁷⁸

Differential diagnosis from CMV and other viral pneumonias is an important consideration, CMV pneumonia usually begins in the parahilar regions in contradistinction to COVID-19 infection, which is more peripheral. During the late stage of dense consolidation with air bronchogram, the differential diagnosis from bacterial pneumonia is important, but the bacterial organisms, which cause dense consolidation, such as *Staphylococcus* and *Klebsiella*, cause edema of the involved lobes, with bulging of fissures and pleural

involvement. Differentiation from hydrostatic pulmonary edema is relevant if septal thickening predominates.⁷⁹

The diagnosis is confirmed by a reverse-transcription polymerase chain reaction test from a nasopharyngeal/oropharyngeal swab or other respiratory fluids.⁷⁹ **Clear guidelines about management of COVID-19 are outlined by WHO and individual country-wise health administrative agencies.** Initial triage into mild, moderate, and severe categories should be performed based on clinical parameters. Supportive therapy includes respiratory care (high flow nasal oxygen, noninvasive, and invasive mechanical ventilation), use of anti-inflammatory agents (corticosteroids, anti-interleukin-6 agents, etc.), antiviral agents (including several repositioned and investigational agents), thromboprophylaxis, and careful follow-up.⁸⁰

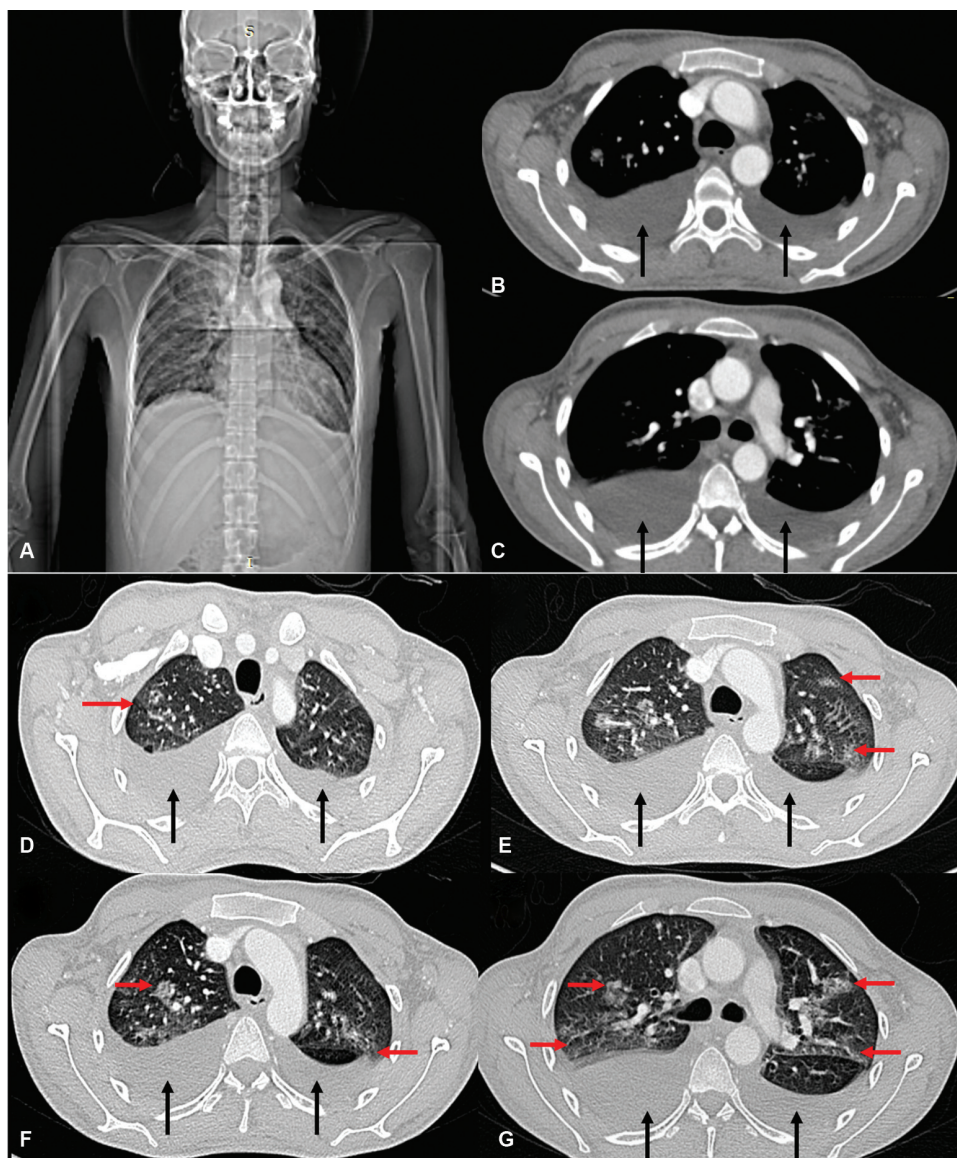


Fig. 22 Thoracic and paranasal sinus imaging of a 20-year-old male, with lymphoma, febrile neutropenia, oronasal skin edema, for the last 2 days. Scout view, mediastinal windows (A–C) show bilateral upper zone infiltrates, pleural effusion (black arrows). Lung windows (D–G) show multiple wedge shaped and nodular ground-glass opacities (red arrows), intermixed with reticular pattern. Paranasal sinuses (H, I) show inflammation in oronasal soft tissue and sinusitis (yellow arrow). Abdominal scans (J, K), show GB and bowel wall thickening (white arrows). Diffuse lung changes with diffuse mucositis suggest cytomegalovirus infection, which was confirmed by relevant serological tests.

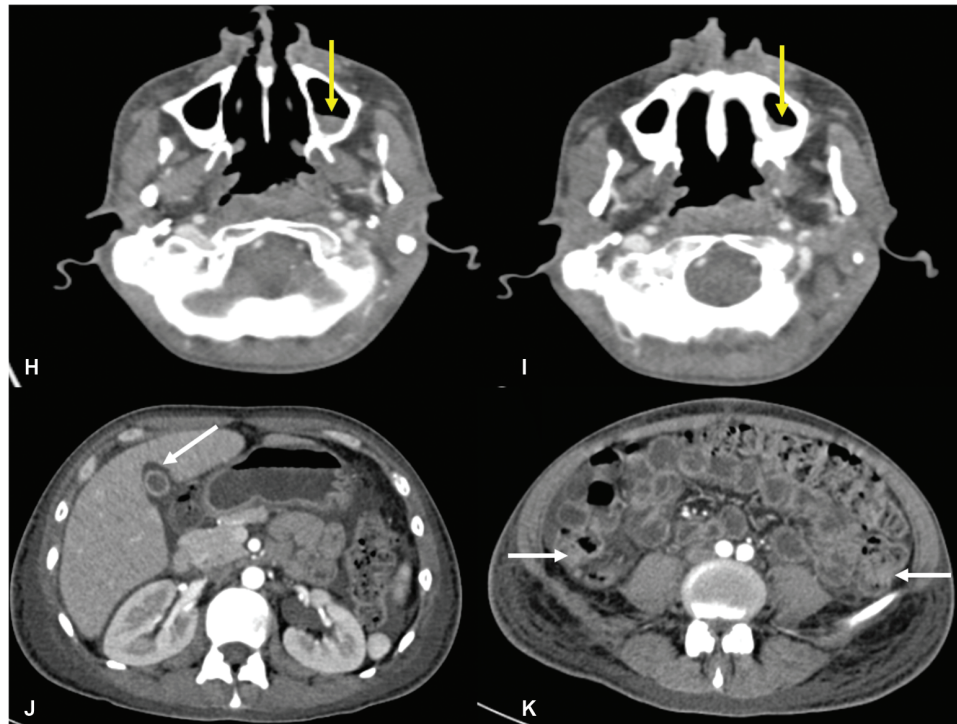


Fig. 22 (Continued)

Parasitic Infections in Immunocompromised Patients

Parasitic infections may occur due to *Toxoplasma gondii* or due to *Strongyloides stercoralis*, but these are rather rare entities and worthy of documentation in case reports.

Toxoplasmosis is a protozoan parasite that infects almost one-third of the world's population. The infection is acquired by ingestion of food or water contaminated by oocytes shed by cats, or by consumption of undercooked infected meat. The primary infection remains subclinical, but manifests as cerebral or ocular or pulmonary toxoplasmosis in immunocompromised patients. **The infection occurs in HIV patients with CD-4 counts below 100 cells/mm³ and is an AIDS defining illness. Besides HIV, transplant patients are also prone to reactivation and invasive disease.** The clinical symptoms are of slow weight loss and low-grade fever for few months that suddenly progress to moderate grade pyrexia, cough and dyspnea, within few days or a week. **The patients have hepatosplenomegaly and peripheral lymphadenopathy.** The clinically worsened state then shows a rapid deterioration to respiratory distress and necessity of ventilatory support, despite emergently instituted broad-based aggressive empiric treatment, which covers the range of community acquired pneumonia, PJP, and viral infections.⁸¹⁻⁸³

Imaging appearances: Lower lobe predominant bilateral GGOs with atelectasis are usually present. These appearances are nonspecific, but the presence of **coexisting ocular and/or brain lesions with peripheral lymphadenopathy and hepatosplenomegaly clinches the diagnosis.**⁸¹⁻⁸³

Differential diagnosis are other causes of lower lobe consolidation like CAP, aspiration pneumonia, and CMV pneumonia. The important clues are clinical background of

HIV and rapid deterioration despite broad-spectrum antimicrobial coverage. The active role of the radiologist is not only to confirm *Toxoplasma gondii* infection but also to correlate the findings with brain and orbit imaging with CT or preferably magnetic resonance imaging in the same sitting, when the patient is sent primarily for pulmonary evaluation.⁸¹⁻⁸³

The diagnosis is confirmed by serological or histological tests demonstrating tachyzoites in BAL fluid/body fluids or tissue samples obtained through TBLB.⁸¹⁻⁸³ **Treatment** of toxoplasmosis is with sulfadiazine and pyrimethamine.⁸¹⁻⁸³

Strongyloides stercoralis Infection

Clinical background: *S. Stercoralis* is a nematode that infects humans through skin contact with larva infested soil. Africa, South America, and Asia are regions of high endemicity, due to poor sanitary conditions. **The hyperinfection syndrome or disseminated strongyloidiasis occur when chronically infected patients are immunosuppressed, especially with diabetes, advanced age, or steroids.** This results in overproliferation of larvae, with dissemination to lungs, liver, and brain. There is rapid onset of fever, cough, hemoptysis, and wheezing, with progression to acute respiratory failure. There is simultaneous development of gastrointestinal disturbances: vomiting, diarrhea, and abdominal pain. Early onset sepsis, secondary bacterial infection, and respiratory failure are the unfortunate eventualities.⁸⁴⁻⁸⁶

Imaging studies with radiographs and CT reveal **parahilar or diffuse GGOs with interlobular septal thickening, resulting in a "crazy-paving" appearance. Less commonly micronodules/military opacities may be encountered. Bilateral pleural effusion is common.** Multiple air-fluid levels in the small bowel are incidentally seen in chest radiographs

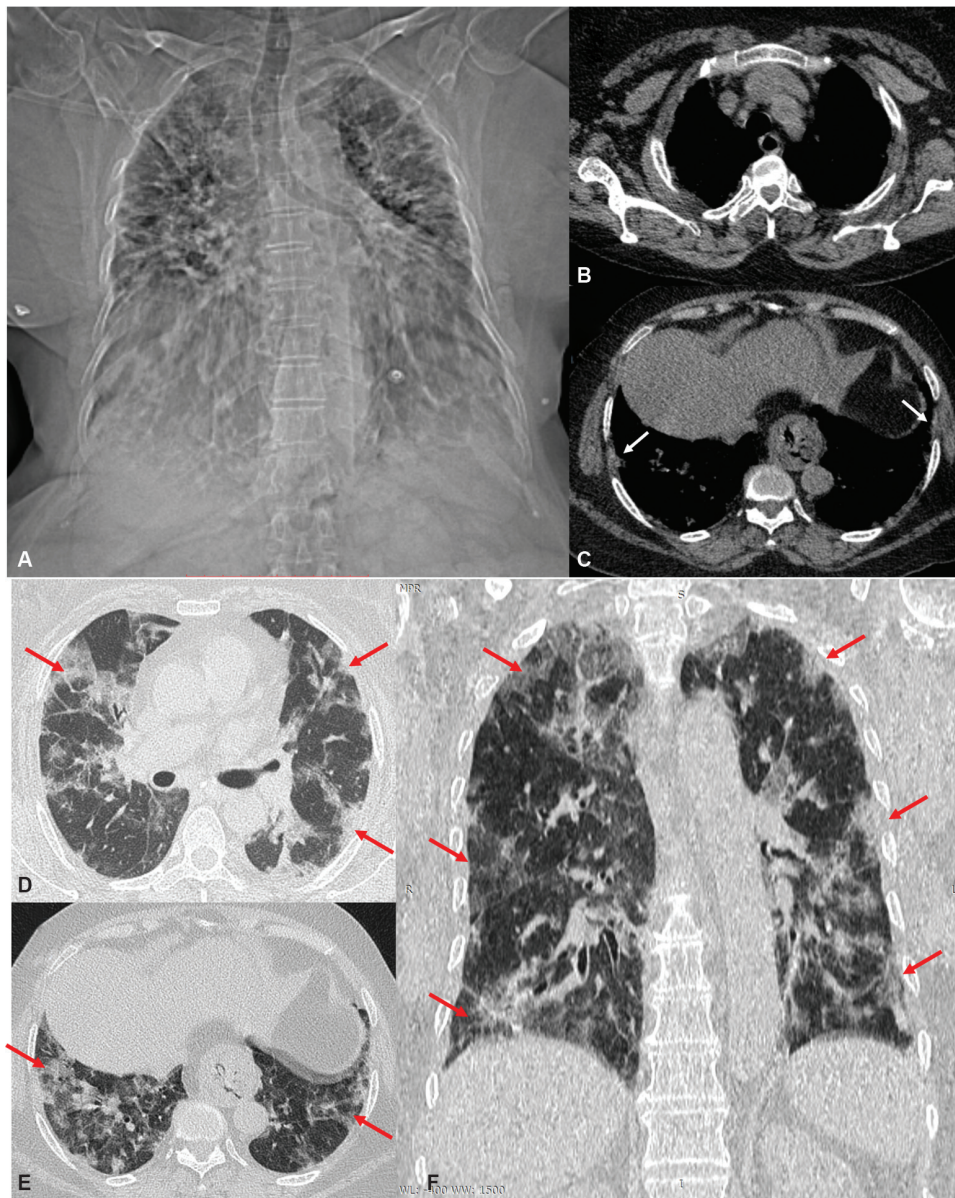


Fig. 23 Computed tomography (CT) of a 71-year-old female, with diabetes, hypertension, fever, progressive breathlessness, for the last 1 week. CT scout view (A) shows cardiomegaly and bilateral reticulonodular shadows. Mediastinal windows (B, C) show subpleural location of few nodular opacities (white arrows). Lung windows (D–F) show multiple, bilateral wedge-shaped ground-glass opacities, majorly in peripheral location, with interspersed reticular pattern (red arrows). Appearances are characteristic for coronavirus disease 2019 infection. The diagnosis confirmed by reverse transcription polymerase chain reaction test on nasopharyngeal–oropharyngeal swab.

due to associated ileus. The clinical clue to parasitic infection, just as in the case of Toxoplasmosis, is a rapid deterioration to respiratory distress and necessity toward ventilatory support, despite emergently instituted broad-spectrum empiric antibiotic treatment, which covers the range of community acquired pneumonia, PJP, and viral infections. **In case of *Strongyloides*, the simultaneous onset of gastrointestinal disturbances is an additional clue.**^{84–86}

Differential diagnosis is from CMV and toxoplasmosis and ARDS. Parahilar opacities with crazy paving and mosaic perfusion favor CMV, on the other hand, associated CNS involvement, lymphadenopathy, and hepatosplenomegaly favor toxoplasmosis, whereas associated bowel disturbances favor *Strongyloides*. Acute phase ARDS, on the other hand,

shows ground-glass opacification that has a characteristic and demonstrable gravitational gradient, as the pathology is distinctly located in the most dependent regions, which are surrounded by normal or hyperinflated lung in the nondependent regions.^{84–86}

The diagnosis is confirmed by stool examination for larvae and demonstration of larvae on histopathology of BAL fluid or TBLB.^{84–86} **Treatment** for strongyloidiasis includes ivermectin, thiabendazole, and albendazole.^{84–86}

Algorithmic Approach toward Pulmonary Infections in Immunocompromised Patients

Radiologists need to dedicatedly correlate the clinical setting, the associated abnormalities, and discriminant imaging

features, to be able to arrive at a fairly accurate etiological diagnosis. The imaging approach based on a “pattern of abnormalities in a typical clinical setting” is summarized below and in the flowchart (→Fig. 24).

Pattern: Lobar consolidation indicates bacterial infection with *Staphylococcus*, *Klebsiella*, or *Pseudomonas*.

Clinical setting is of an acute onset of disease. A majority of patients who are diabetic, alcoholic, chronic kidney disease and those of elderly age group are more likely to be infected with bacterial infections (often mixed) by agents such as *Staphylococcus*, *Klebsiella*, *Pseudomonas*, *Legionella*, and *H. influenzae*. *Staphylococcus* and *Klebsiella* both show lobar consolidation and cause lung edema with bulging fissures. The presence of bilateral empyema, pneumatocele, and pneumothorax is in favor of *Staphylococcus*. Both these organisms may cause deterioration to necrotizing pneumonia and vasculopathy.

Pattern: Mixed, with patchy consolidation, GGOs and bronchial wall thickening with centrilobular nodules indicate a bacterial infection with *H. influenzae* or *Mycoplasma*.

Clinical setting is of acute onset disease that occurs in *H. influenzae*, which is more common in diabetics, smokers, and in patients with preexisting COPD. However, *Mycoplasma* has more of a subacute onset. *H. influenzae* and *Mycoplasma* both present a mixed picture with GGO, patchy consolidation, and nodular opacities. Mixed bacterial infections are also likely in aspiration pneumonia, in ICU and ventilator-acquired pneumonia and there is a greater likelihood of their being multidrug resistant and progressing to necrotizing pneumonia and acute respiratory failure.

Pattern of consolidation: Multiple lung segments involved, then aspiration pneumonia complicated by mixed bacterial infections is likely. The organisms causing aspiration pneumonia are the same as for CAP or HAP: *Pseudomonas*, *Klebsiella*, *E. coli*, and *Staphylococcus*.

Clinical setting is of an acute onset disease. Patients with depressed immunity such as alcoholics and diabetic patients with cerebrovascular disease and stroke/stroke sequelae are prone to aspiration pneumonia. If multiple lung segments are involved, then the **likelihood of drug resistance, ARDS, necrotizing pneumonia, and lung gangrene increases.**

Pattern: Mixed, with patchy consolidation, GGOs and bronchial wall thickening with centrilobular nodules and fibroses all occurring together, indicates *Mycobacterium tuberculosis* infection.

Clinical history: Subacute or chronic onset disease. Tuberculosis is common among diabetics, patients on prolonged steroid therapy, and HIV-infected individuals. This pattern is of a postprimary (tubercular) disease. Coexisting lymphadenopathy and pleural effusion are the rule. **Associated liver, spleen invasion, and abdominal lymphadenopathy should be diligently assessed as the patient prognosis is affected by disseminated disease. Differential diagnosis includes subacute and chronic fungal infections like mucormycosis, histoplasmosis, and *Cryptococcus*.**

Pattern: Miliary lesions, with multiorgan dissemination: also indicates a *Mycobacterium tuberculosis* infection.

Clinical setting is of an acute onset disease. Severe immunosuppression in HIV or prolonged steroid therapy with falling CD-4 counts below 200 cells/mm³. Tuberculosis in diabetics and in HIV tends to be more aggressive and disseminated than in immunocompetent individuals. **Associated miliary lesions in liver and spleen are very likely and should be excluded, as the patient prognosis is affected by disseminated disease.** Differential diagnosis of miliary lesions includes viral infections (Herpes family) and fungal infections such as histoplasmosis.

Pattern: Multiple macronodules, with ill-defined borders and a halo sign or a reverse halo sign with multiple GGOs: diagnosis is acute angioinvasive fungal infection. In immunocompromised patients, the angioinvasive fungal infections are commonly due to *Aspergillus* and *Candida*.

Clinical setting is of an acute onset febrile neutropenia. Fungal infections of the angioinvasive kind occur in patients with hematological malignancy, solid organ transplant, febrile neutropenia, HIV patients, and in those on prolonged steroid therapy. **Associated liver and spleen invasion should be excluded, as the patient prognosis is affected by disseminated disease. Differential diagnosis is from mucormycosis, which is more frequent in diabetics, has more peripheral lesions, and often shows reverse halo sign.**

Pattern: Patchy consolidation, nodules, and cavitation all present together, just like in chronic postprimary tuberculosis: diagnosis is chronic fungal infection.

Clinical setting: Subacute or chronic onset disease. Chronic fungal infections are common in diabetics, chronic alcoholics, malnourished individuals and with prolonged steroid therapy and in patients with HIV. *Aspergillus* and *Candida* may infect as a chronic form, other than an angioinvasive form. The imaging appearances are of patchy consolidation, nodules, and cavitation all present together, just like in chronic post-primary tuberculosis. Associated liver and spleen involvement is likely. Histoplasmosis is associated with mucocutaneous lesions and adrenal involvement, other than liver and spleen, which are the important clues to its diagnosis. In a patient with poorly controlled diabetes, the associated orbital and rhinocerebral lesions and GIT involvement favor mucormycosis infection. In case only brain lesions are present with a mixed pattern of lung lesions, especially with a low CD-4 count in immunosuppressed solid organ transplant or HIV patients, then *Cryptococcus* is the likely agent. Blastomycoses, on the other hand, are more likely in patients who are residents of endemic belts in North America and associated skin lesions are a clue.

Pattern: Diffuse GGOs, likely diagnosis is *P. jirovecii*, CMV pneumonia, COVID-19 infection, or parasitic infestation of lungs.

Clinical setting is of an acute onset disease with rapid deterioration to respiratory failure. *P. jirovecii* infection is a fungal infection that is common in AIDS, solid organ

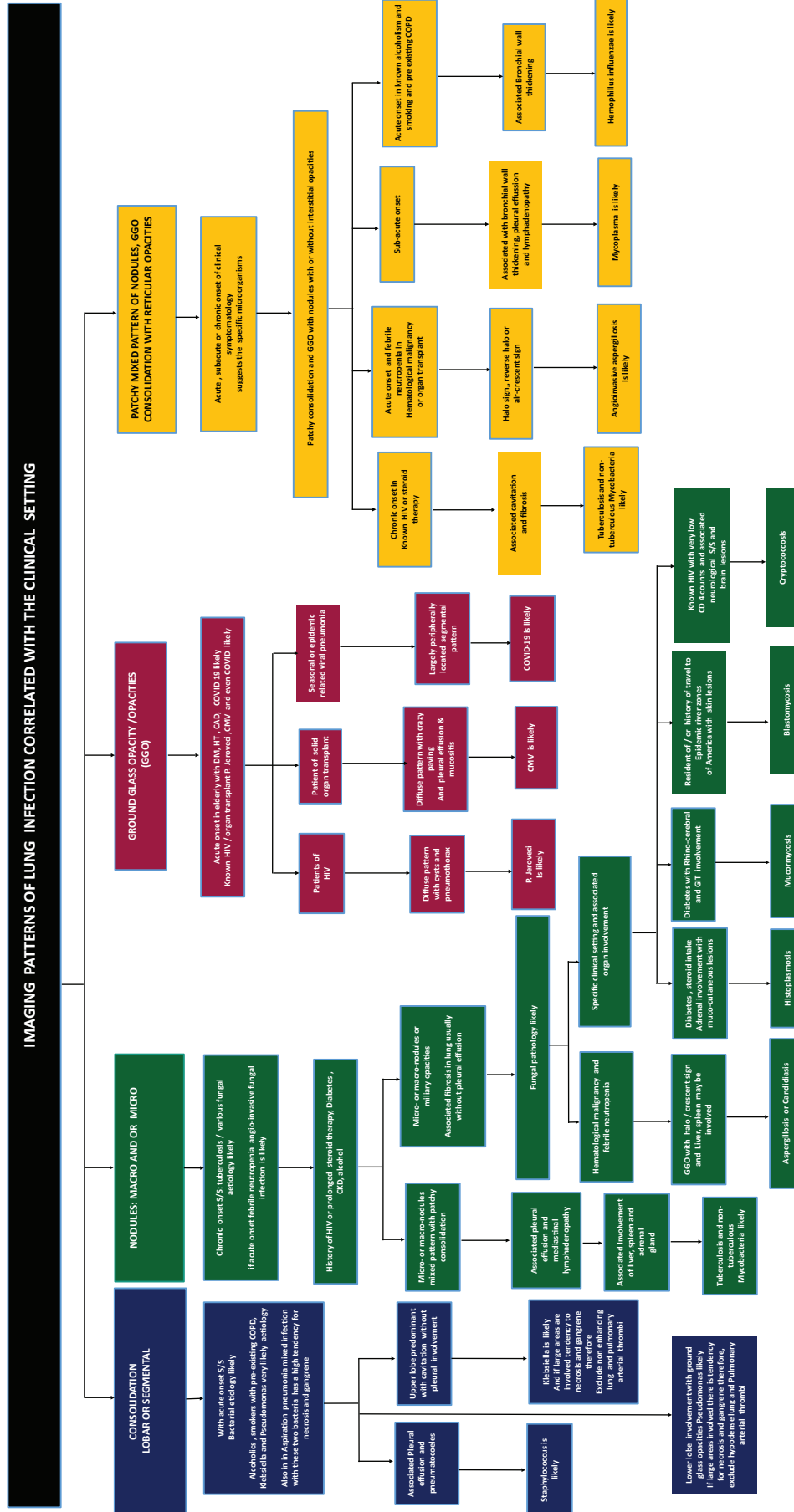


Fig. 24 Flow chart, summarizing the pattern-based approach, effectively amalgamated with clinical correlation, for arriving at an imaging diagnosis of the most likely aetiology of pulmonary infection in immunocompromised patients.

transplant and patients of hematological malignancy and ICU patients. Diffuse GGO with **cysts and a tendency to pneumothorax are signature imaging features.**

Clinical setting: CMV infection may occur in HIV patients with low CD-4 counts or in severely immunosuppressed solid organ transplant patients. CT shows a pattern of bilateral, predominantly **parahilar GGOs, but these are usually superimposed with an interstitial pattern of thickened interlobular septa and septal thickening, which renders a “crazy paving” appearance.**

Clinical setting: COVID-19 infection can be disastrous in diabetic patients and these also present with multiple but **peripheral GGO, may occur with reverse halo sign, which rapidly progress to diffuse opacification,** subsequently to extensive consolidation, pleural thickening, and acute respiratory failure. Vascular involvement is likely in COVID-19 infection and may necessitate a CTPA.

Parasitic infections in immunocompromised patients are rare and should be considered in patients of solid organ transplant, who **rapidly develop fever, respiratory distress, and hemoptysis and do not respond to broad-spectrum antimicrobial therapy. Associated abdominal complaints and ileus are important clues to etiology** of strongyloides infection whereas, the presence of hepatosplenomegaly associated with lymphadenopathy suggests toxoplasmosis as the aetiological agent.

Conclusion

Although the final diagnosis is confirmed by isolating the offending organism from blood, sputum, respiratory tract secretions, or BAL aspirate or lung biopsy or pleural aspirate, nevertheless the role of the radiologist remains paramount not only in documenting the presence of disease, but also its extent, also for suggesting the most likely aetiological agent and for the prognostication, based on the sites and number of extra pulmonary organs involved. Diligent planning and execution of the radiological examination can swing the diagnosis in conditions such as disseminated tuberculosis, and disseminated histoplasmosis, as much as it can in necrotizing pneumonia or in angioinvasive fungal infection or COVID-19 infection necessitating a CT angiography study. **A thorough knowledge of characteristic imaging patterns can fairly accurately narrow down the differential diagnoses, especially when correlated with the known typical clinical setting and the characteristic abnormalities in other organ systems/body structures.** Furthermore, the narrowed differential diagnosis provided by imaging studies not only accurately steers the subsequent laboratory evaluation but also pinpoints the ideal sites for sampling of tissues and/or fluids for confirmatory tests. Therefore, the role of the radiologist as a vital member in the frontline team for management of lung infections, in the case of immunocompromised patients, remains undeniably paramount.

Conflicting Interest

None declared.

References

- Vazquez Guillamet C, Hsu JL, Dhillon G, Vazquez Guillamet R. Pulmonary infections in immunocompromised hosts: Clinical. *J Thorac Imaging* 2018;33(05):295–305
- Oh YW, Effmann EL, Godwin JD. Pulmonary infections in immunocompromised hosts: the importance of correlating the conventional radiologic appearance with the clinical setting. *Radiology* 2000;217(03):647–656
- Vaillant A, Qurie A. Immunodeficiency [Internet]. Ncbi. nlm.nih.gov 2020 [cited 14 July 2020]. Accessed January 30, 2022 from: <https://www.ncbi.nlm.nih.gov/books/NBK500027/>
- Peck K, Kim T, Lee M, Lee K, Han J. Pneumonia in immunocompromised patients: updates in clinical and imaging features. *Precision Future Med* 2018;2(03):95–108
- Bajaj SK, Tombach B. Respiratory infections in immunocompromised patients: lung findings using chest computed tomography. *Radiol Infect Dis* 2017;4(01):29–37
- Sarkar D, Jung MK, Wang HJ. Alcohol and the immune system. *Alcohol Res* 2015;37(02):153–155
- Berbudi A, Rahmadika N, Tjahjadi AI, Ruslami R. Type 2 diabetes and its impact on the immune system. *Curr Diabetes Rev* 2020;16(05):442–449
- Syed-Ahmed M, Narayanan M. Immune dysfunction and risk of infection in chronic kidney disease. *Adv Chronic Kidney Dis* 2019;26(01):8–15
- França T, Ishikawa L, Zorzella-Pezavento S, Chiuso-Minicucci F, da Cunha M, Sartori A. Impact of malnutrition on immunity and infection. *J Venom Anim Toxins Incl Trop Dis* 2009;15(03):374–390
- Fuentes E, Fuentes M, Alarcón M, Palomo I. Immune system dysfunction in the elderly. *An Acad Bras Cienc* 2017;89(01):285–299
- Meidani M, Naeini AE, Rostami M, Sherkat R, Tayeri K. Immunocompromised patients: review of the most common infections happened in 446 hospitalized patients. *J Res Med Sci* 2014;19(Suppl 1):S71–S73
- Ahuja J, Kanne JP. Thoracic infections in immunocompromised patients. *Radiol Clin North Am* 2014;52(01):121–136
- Azoulay E, Russell L, Van de Louw A, et al; Nine-i Investigators. Diagnosis of severe respiratory infections in immunocompromised patients. *Intensive Care Med* 2020;46(02):298–314
- Soldati G, Smargiassi A, Inchingolo R, et al. Proposal for international standardization of the use of lung ultrasound for patients with COVID-19: a simple, quantitative, reproducible method. *J Ultrasound Med* 2020;39(07):1413–1419
- Tanaka N, Kunihiro Y, Yanagawa N. Infection in immunocompromised hosts: imaging. *J Thorac Imaging* 2018;33(05):306–321
- Kunihiro Y, Tanaka N, Kawano R, et al. Differential diagnosis of pulmonary infections in immunocompromised patients using high-resolution computed tomography. *Eur Radiol* 2019;29(11):6089–6099
- Kulkarni AP, Sengar M, Chinnaswamy G, et al. Indian antimicrobial prescription guidelines in critically ill immunocompromised patients. *Indian J Crit Care Med* 2019;23(Suppl 1):S64–S96
- Mahendra M, Jayaraj BS, Lokesh KS, et al. Antibiotic prescription, organisms and its resistance pattern in patients admitted to respiratory ICU with respiratory infection in Mysuru. *Indian J Crit Care Med* 2018;22(04):223–230
- Baldassarri RJ, Kumar D, Baldassarri S, Cai G. Diagnosis of infectious diseases in the lower respiratory tract: a cytopathologist's perspective. *Arch Pathol Lab Med* 2019;143(06):683–694

- 20 Geake J, Hammerschlag G, Nguyen P, et al. Utility of EBUS-TBNA for diagnosis of mediastinal tuberculous lymphadenitis: a multicentre Australian experience. *J Thorac Dis* 2015;7(03):439–448
- 21 Murdoch DR, Werno AM, Jennings LC. Microbiological; diagnosis of respiratory illness: recent advances. In: Chernick V, Kendig E, eds. *Kendig's Disorders of the Respiratory Tract in Children*. 9th edition New York: Elsevier; 2018:396–405
- 22 Washington JA. Principles of diagnosis. In: Baron S, ed. *Medical Microbiology*. 4th edition Galveston (TX): University of Texas Medical Branch at Galveston; 1996. Chapter 10. Accessed January 30, 2022 from: <https://www.ncbi.nlm.nih.gov/books/NBK8014/>
- 23 Stanzani M, Sassi C, Lewis RE, et al. High resolution computed tomography angiography improves the radiographic diagnosis of invasive mold disease in patients with hematological malignancies. *Clin Infect Dis* 2015;60(11):1603–1610
- 24 Chen C (August 29th 2011) *Gangrenous Lung Disease, Gangrene - Current Concepts and Management Options*, Alexander Vitin, IntechOpen. . Doi: 10.5772/22495. Accessed January 30, 2022 from: <https://www.intechopen.com/books/gangrene-current-concepts-and-management-options/gangrenous-lung-disease>
- 25 Hansell DM, Bankier AA, MacMahon H, McLoud TC, Müller NL, Remy J. *Fleischner Society: glossary of terms for thoracic imaging*. *Radiology* 2008;246(03):697–722
- 26 Okada F, Ando Y, Tanoue S, et al. Radiological findings in acute *Haemophilus influenzae* pulmonary infection. *Br J Radiol* 2012;85(1010):121–126
- 27 Mane A, Gujar P, Gaikwad S, et al. Aetiological spectrum of severe community-acquired pneumonia in HIV-positive patients from Pune, India. *Indian J Med Res* 2018;147(02):202–206
- 28 Miyashita N, Sugiu T, Kawai Y, et al. Radiographic features of *Mycoplasma pneumoniae* pneumonia: differential diagnosis and performance timing. *BMC Med Imaging* 2009;9(01):7
- 29 Okada F, Ono A, Ando Y, et al. Thin-section CT findings in *Pseudomonas aeruginosa* pulmonary infection. *Br J Radiol* 2012;85(1020):1533–1538
- 30 Musher DM, Thorner AR. Community-acquired pneumonia. *N Engl J Med* 2014;371(17):1619–1628
- 31 Shindo Y, Ito R, Kobayashi D, et al. Risk factors for drug-resistant pathogens in community-acquired and healthcare-associated pneumonia. *Am J Respir Crit Care Med* 2013;188(08):985–995
- 32 Sanivarapu R, Gibson J. *Aspiration Pneumonia* [Internet]. *Ncbi.nlm.nih.gov* 2020 [cited 11 July 2020]. Accessed January 30, 2022 from: <https://www.ncbi.nlm.nih.gov/books/NBK470459/>
- 33 Mandell LA, Niederman MS. *Aspiration pneumonia*. *N Engl J Med* 2019;380(07):651–663
- 34 Chatha N, Fortin D, Bosma KJ. Management of necrotizing pneumonia and pulmonary gangrene: a case series and review of the literature. *Can Respir J* 2014;21(04):239–245
- 35 Nachiappan AC, Rahbar K, Shi X, et al. Pulmonary tuberculosis: role of radiology in diagnosis and management. *Radiographics* 2017;37(01):52–72
- 36 Bächler P, Baladron MJ, Menias C, et al. Multimodality imaging of liver infections: differential diagnosis and potential pitfalls. *Radiographics* 2016;36(04):1001–1023
- 37 van Haren Noman S, Visser H, Muller AF, Limonard GJM. Addison's disease caused by tuberculosis: diagnostic and therapeutic difficulties. *Eur J Case Rep Intern Med* 2018;5(08):000911. Doi: 10.12890/2018_00091
- 38 Grover SB, Midha N, Gupta M, Sharma U, Talib VH. Imaging spectrum in disseminated histoplasmosis: case report and brief review. *Australas Radiol* 2005;49(02):175–178
- 39 Sharma S, Singh P, Sahu KK, Rajwanshi A, Malhotra P, Naseem S. Histoplasmosis in pleural effusion in a 23-year-old man with mixed-phenotype acute leukemia. *Lab Med* 2017;48(03):249–252
- 40 WHO Consolidated Guidelines on Tuberculosis. Module 4: Treatment - Drug-Resistant Tuberculosis Treatment [Internet]. *Who.int* 2020 [cited 11 August 2020]. Accessed January 30, 2022 from: <https://www.who.int/publications/i/item/9789240007048>
- 41 [Internet] *Tbcindia.gov.in*. 2020 [cited 11 August 2020]. Accessed January 30, 2022 from: <https://tbcindia.gov.in/WriteReadData/NSP%20Draft%2020.02.2017%201.pdf>
- 42 Franquet T, Giménez A, Hidalgo A. Imaging of opportunistic fungal infections in immunocompromised patient. *Eur J Radiol* 2004;51(02):130–138
- 43 Gopalakrishnan R, Nambi PS, Ramasubramanian V, Abdul Ghafur K, Parameswaran A. Histoplasmosis in India: truly uncommon or uncommonly recognised? *J Assoc Physicians India* 2012;60:25–28
- 44 George P, Nayak N, Anoop TM, Gopi N, Vikram HP, Sankar A. Pulmonary histoplasmosis mimicking carcinoma lung. *Lung India* 2015;32(06):663–665
- 45 Truong J, Ashurst JV. *Pneumocystis (Carinii) Jiroveci Pneumonia*. Treasure Island, FL: Stat Pearls Publishing; 2020
- 46 Li MC, Lee NY, Lee CC, Lee HC, Chang CM, Ko WC. *Pneumocystis jiroveci pneumonia in immunocompromised patients: delayed diagnosis and poor outcomes in non-HIV-infected individuals*. *J Microbiol Immunol Infect* 2014;47(01):42–47
- 47 McBride JA, Gauthier GM, Klein BS. Clinical manifestations and treatment of blastomycosis. *Clin Chest Med* 2017;38(03):435–449
- 48 Randhawa HS, Chowdhary A, Kathuria S, et al. Blastomycosis in India: report of an imported case and current status. *Med Mycol* 2013;51(02):185–192
- 49 Greene R. The radiological spectrum of pulmonary aspergillosis. *Med Mycol* 2005;43(Suppl 1):S147–S154
- 50 Kawashima A, Kuhlman JE, Fishman EK, et al. Pulmonary Aspergillus chest wall involvement in chronic granulomatous disease: CT and MRI findings. *Skeletal Radiol* 1991;20(07):487–493
- 51 Franquet T, Müller NL, Lee KS, Oikonomou A, Flint JD. Pulmonary candidiasis after hematopoietic stem cell transplantation: thin-section CT findings. *Radiology* 2005;236(01):332–337
- 52 Orłowski HLP, McWilliams S, Mellnick VM, et al. Imaging spectrum of invasive fungal and fungal-like infections. *Radiographics* 2017;37(04):1119–1134
- 53 Davda S, Kowa XY, Aziz Z, et al. The development of pulmonary aspergillosis and its histologic, clinical, and radiologic manifestations. *Clin Radiol* 2018;73(11):913–921
- 54 Althoff Souza C, Müller NL, Marchiori E, Escuissato DL, Franquet T. Pulmonary invasive aspergillosis and candidiasis in immunocompromised patients: a comparative study of the high-resolution CT findings. *J Thorac Imaging* 2006;21(03):184–189
- 55 Georgiadou SP, Sipsas NV, Marom EM, Kontoyiannis DP. The diagnostic value of halo and reversed halo signs for invasive mold infections in compromised hosts. *Clin Infect Dis* 2011;52(09):1144–1155
- 56 Maturu VN, Agarwal R. Reversed halo sign: a systematic review. *Respir Care* 2014;59(09):1440–1449
- 57 Yeom SK, Kim HJ, Byun JH, Kim AY, Lee MG, Ha HK. Abdominal aspergillosis: CT findings. *Eur J Radiol* 2011;77(03):478–482
- 58 Sherif R, Segal BH. Pulmonary aspergillosis: clinical presentation, diagnostic tests, management and complications. *Curr Opin Pulm Med* 2010;16(03):242–250
- 59 Jairam A, Dassi M, Chandola P, Lall M, Mukherjee D, Hooda AK. *Pneumocystis jiroveci outbreak in a renal transplant center: Lessons learnt*. *Indian J Nephrol* 2014;24(05):276–279
- 60 Udwardia ZF, Doshi AV, Bhaduri AS. *Pneumocystis carinii pneumonia in HIV infected patients from Mumbai*. *J Assoc Physicians India* 2005;53:437–440
- 61 Kanne JP, Yandow DR, Meyer CA. *Pneumocystis jiroveci pneumonia: high-resolution CT findings in patients with and without HIV infection*. *AJR Am J Roentgenol* 2012;198(06):W555–61. Doi: 10.2214/AJR.11.7329
- 62 Bukamur HS, Kareem E, Fares S, Al-Ourani M, Al-Astal A. *Pneumocystis jirovecii (carinii) pneumonia causing lung cystic lesions and*

- pneumomediastinum in non-HIV infected patient. *Respir Med Case Rep* 2018;25:174–176
- 63 Nasnas R, Matta MY, El Helou G, Rizk N, Sarkis DK, Moussa R. Brain abscesses in HIV-positive patients due to *Pneumocystis jirovecii*. *J Int Assoc Physicians AIDS Care (Chic)* 2012;11(03):169–171
- 64 Lum J, Abidi ZM, McCollister B, Henao-Martínez A. Miliary histoplasmosis in a patient with rheumatoid arthritis. *Case Rep Med* 2018;2018:1–6
- 65 Agrawal R, Yeldandi A, Savas H, Parekh ND, Lombardi PJ, Hart EM. Pulmonary mucormycosis: risk factors, radiologic findings, and pathologic correlation. *Radiographics* 2020;40(03):656–666
- 66 Challa S, Uppin SG, Uppin MS, Paul RT, Prayaga AK, Rao MT. Pulmonary zygomycosis: a clinicopathological study. *Lung India* 2011;28(01):25–29
- 67 Zhang Y, Li N, Zhang Y, et al. Clinical analysis of 76 patients pathologically diagnosed with pulmonary cryptococcosis. *Eur Respir J* 2012;40(05):1191–1200
- 68 Saag MS, Graybill RJ, Larsen RA, et al; Infectious Diseases Society of America. Practice guidelines for the management of cryptococcal disease. *Clin Infect Dis* 2000;30(04):710–718
- 69 Maini R, Ranjha S, Tandan N, et al. Pulmonary blastomycosis: a case series and review of unique radiological findings. *Med Mycol Case Rep* 2020;28:49–54
- 70 Franquet T. Imaging of pneumonia: trends and algorithms. *Eur Respir J* 2001;18(01):196–208
- 71 Franquet T. Imaging of pulmonary viral pneumonia. *Radiology* 2011;260(01):18–39
- 72 Moon JH, Kim EA, Lee KS, Kim TS, Jung KJ, Song JH. Cytomegalovirus pneumonia: high-resolution CT findings in ten non-AIDS immunocompromised patients. *Korean J Radiol* 2000;1(02):73–78
- 73 Tan BH. Cytomegalovirus treatment. *Curr Treat Options Infect Dis* 2014;6(03):256–270
- 74 Carotti M, Salaffi F, Sarzi-Puttini P, et al. Chest CT features of coronavirus disease 2019 (COVID-19) pneumonia: key points for radiologists. *Radiol Med (Torino)* 2020;125(07):636–646
- 75 Apicella M, Campopiano MC, Mantuano M, Mazoni L, Coppelli A, Del Prato S. COVID-19 in people with diabetes: understanding the reasons for worse outcomes. *Lancet Diabetes Endocrinol* 2020;8(09):782–792
- 76 Patel RH, Pella PM. COVID-19 in a patient with HIV infection. [published online ahead of print, 2020 May 22] *J Med Virol* 2020;92(11):2356–2357. Doi: 10.1002/jmv.26049.doi:10.1002/jmv.26049
- 77 Pan F, Ye T, Sun P, et al. Time course of lung changes on chest CT during recovery from 2019 novel coronavirus (COVID-19) pneumonia. *Radiology* 2020;295:715–721 <https://doi.org/10.1148/radiol.2020200370>
- 78 Prokop M, van WEVERDINGEN, van TREES Vellinga, et al. CO-RADS: A Categorical CT Assessment Scheme for Patients Suspected of Having COVID-19-Definition and Evaluation. *Radiology* 2020;296(02):E97E104
- 79 Dai WC, Zhang HW, Yu J, et al. CT imaging and differential diagnosis of COVID-19. *Can Assoc Radiol J* 2020;71(02):195–200
- 80 [Internet] Mohfw.gov.in. 2020 [cited 11 August 2020]. Accessed January 30, 2022 from: <http://www.mohfw.gov.in/pdf/Updated-ClinicalManagementProtocolforCOVID19dated03072020.pdf>
- 81 Garg D, Madan N, Qaqish O, Nagarakanti S, Patel V. Pulmonary toxoplasmosis diagnosed on transbronchial lung biopsy in a mechanically ventilated patient. *Case Rep Infect Dis* 2020;2020:97101825
- 82 Velásquez JN, Ledesma BA, Nigro MG, et al. Pulmonary toxoplasmosis in human immunodeficiency virus-infected patients in the era of antiretroviral therapy. *Lung India* 2016;33(01):88–91
- 83 Remington JS, Thulliez P, Montoya JG. Recent developments for diagnosis of toxoplasmosis. *J Clin Microbiol* 2004;42(03):941–945
- 84 Nabeya D, Haranaga S, Parrott GL, et al. Pulmonary strongyloidiasis: assessment between manifestation and radiological findings in 16 severe strongyloidiasis cases. *BMC Infect Dis* 2017;17(01):320
- 85 Bae K, Jeon KN, Ha JY, Lee JS, Na BK. Pulmonary strongyloidiasis presenting micronodules on chest computed tomography. *J Thorac Dis* 2018;10(08):E612–E615
- 86 Dogan C, Gayaf M, Ozsoz A, et al. Pulmonary Strongyloides stercoralis infection. *Respir Med Case Rep* 2014;11:12–15